Materials and methods

Cell culture

Neuro2a (N2a), PC12D, and HeLa cells were grown as previously described [27, 28]. HEK293 cells were grown in Dulbecco's Modified Eagle's Medium (DMEM) (Wako) supplemented with 10% fetal bovine serum (FBS) (Sigma), 100 U/ml penicillin and 100 μg/ml streptomycin (Sigma). F9 cells were grown in DMEM supplemented with 15% FBS and the antibiotics as described above. SH-SY5Y cells were grown in EMEM/F-12 (1:1 mixture) containing 10% FBS and the antibiotics. All the cells were cultured at 37°C in 5% CO_2-humidified chamber. HEK293 (Registry No. JCRB9068) and F9 (Registry No. JCRB0001) cells were purchased from the Health Science Research Resources Bank. SH-SY5Y (Registry No. CRL-2266) cells were purchased from the American Type Culture Collection.

Construction of reporter plasmids

To examine the effects of endogenous *let-7* on gene silencing against its target genes, we constructed reporter plasmids with the psiCHECK-2 plasmid (Promega) carrying the *Renilla* and *Photinus luciferase* genes. The plasmid was digested with *Xho* I and *Pme* I, and subjected to ligation with synthetic oligonucleotide duplexes carrying target sequences for *let-7* (the sequences of the oligonucleotides are indicated below). The resultant plasmids carry perfectly matched target sequence (PMTS) and three bulged binding sites (3xBBS) for *let-7* (Fig. 1). We further constructed reporter plasmids by replacing the Bgl II–Nhe I region containing the simian virus 40 (SV40) promoter in the above plasmids with the Bgl II–Nhe I fragment encoding the herpes simplex virus thymidine kinase (TK) promoter isolated from the phRL-TK plasmid (Promega); the resultant reporter plasmids carry the TK promoter linked with the *Renilla luciferase* gene (Fig. 1).

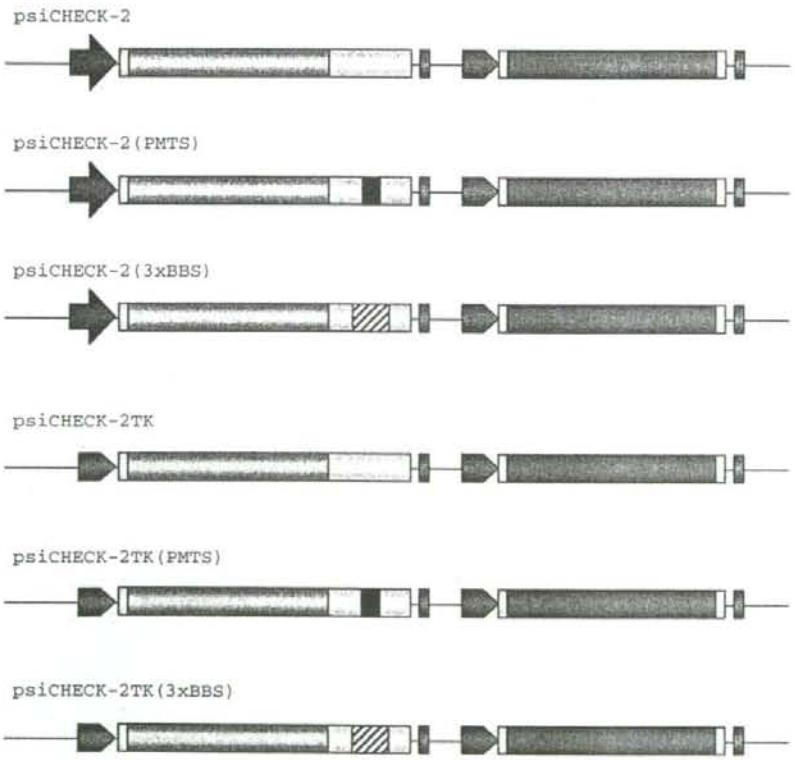

Fig. 1 Constructs of reporter plasmids. Reporter plasmids were constructed based on the psiCHECK-2 plasmid (Promega). Yellow, green, gray and pink boxes indicate the *Renilla* and *Photinus luciferase* coding regions, untranslated region, and poly(A) signal, respectively. Red arrow and orange pentagon indicate the SV40 and TK promoters, respectively. Solid and hatched boxes represent perfectly matched target sequence (PMTS) and three bulged binding sites (3 × BBS) for *let-7*, respectively

The sequences of the oligonucleotides synthesized are as follows:

Ss-let-7(PMTS): 5′-TCGAGAACTATACAACCTACT ACCTCATTACTAGT-3′
As-let-7(PMTS): 5′-ACTAGTAATGAGGTAGTAGGT TGTATAGTTC-3′
Ss-let-7(3 × BBS): 5′-TCGAGGGACAGCCTATTGA ACTACCTCACTCGGAGCACAGCCTATTGAACTAC CTCAGGCCTGCACAGCCTATTGAACTACCTCATT ACTAGT-3′
As-let-7(3 × BBS): 5′-ACTAGTAATGAGGTAGTTC AATAGGCTGTGCAGGCCTGAGGTAGTTCAATAG GCTGTGCTCCGAGTGAGGTAGTTCAATAGGCTGT CCC-3′

Transfection and reporter assay

Transfection of the reporter plasmids was carried out using Lipofectamine 2000 transfection reagent (Invitrogen) according to the manufacturer's instructions, and to each well (24-well culture plates) 0.1 μg of each reporter plasmid was applied. Forty-eight hours after transfection, cell lysate was prepared and the expression levels of luciferases were examined by the Dual-Luciferase reporter assay system (Promega), according to the manufacturer's instructions. The reporter plasmids were also transfected together with either Pre-miR miRNA precursor (Production ID: PM10048; Ambion) or Anti-miR miRNA inhibitor (Production ID: AM10048; Ambion) of *let-7a* into cells, and then the expression of the reporter genes were examined as described above.

Reverse transcription-(real time) polymerase chain reaction (RT-(real time) PCR)

Total RNA was extracted from cells with Trizol reagent (Invitrogen) and subjected to RT-(real time) PCR. Real-time PCR was carried out by means of the AB 7300 Real Time PCR System (Applied Biosystems) with a TaqMan Universal PCR Master Mix together with Assays-on-Demand Gene Expression products (Applied Biosystems) or a SYBR Green PCR Master Mix together with Perfect Real Time Primers (TAKARA BIO), according to the manufacturers' instructions. The Assays-on-Demand Gene Expression products and Perfect Real Time Primers used are shown in Tables 1 and 2, respectively.

To examine the expression levels of *let-7a* and *5sRNA* as a control, total RNA was subjected to RT-PCR using the mirVana qRT-PCR detection kit (Ambion). Real-time PCR was performed by the AB 7300 Real Time PCR system (Applied Biosystems) with SuperTaq polymerase (Ambion). End-point PCR analysis after RT reaction was also carried out by the GeneAmp PCR system 9700 (Applied Biosystems) according to the manufacturer's instructions. The resultant PCR products were electrophoretically separated on 12% polyacrylamide gels and visualized by ethidium bromide staining.

Table 1 Assays-on-demand gene expression products used in this study

Human genes		Mouse genes	
Gene name	Assay ID	Gene name	Assay ID
EIF2C1	Hs00201864_m1	*Eif2c1*	Mm00462977_m1
EIF2C2	Hs00293044_m1	*Eif2c2*	Mm00838341_m1
EIF2C3	Hs00227461_m1	*Eif2c3*	Mm00462959_m1
EIF2C4	Hs00214142_m1	*Eif2c4*	Mm00462659_m1
DICER	Hs00229023_m1	*Zfp36*	Mm00457144_m1
ZFP36	Hs00185658_m1	*Trc6a*	Mm00523487_m1
TRC6A	Hs00379422_m1	*Gapdh*	Mm99999915_g1
GAPDH	Hs99999905_m1		

Table 2 Perfect real time primers used in this study

Human genes		Mouse genes	
Gene name	Primer-Set ID	Gene name	Primer-Set ID
TARBP2	HA039221	*Dicer*	MA043537
PRKRA	HA038462	*Tarbp2*	MA027351
		Prkra	MA030829

DNA chip analysis

Total RNA was extracted from cultured cells using Trizol reagent (Invitrogen). For preparation of cellular miRNAs, small-sized RNAs containing miRNAs were isolated from total RNA using the RNeasy MinElute Cleanup kit (Qiagen). The isolated small-sized RNAs (~1 μg) were subjected to direct labeling with a fluorescent dye using the Platinum*Bright* 647 Infrared nucleic acid labeling kit (KREATECH), according to the manufacturer's instructions. After labeling, the labeled RNAs were purified from free fluorescent substrates by KREA*pure* columns (KREATECH) and used in hybridization. Hybridization was carried out with the *Genopal*®-MICM DNA chips (Mitsubishi Rayon) for detection of mouse miRNAs as described previously [27, 29]. After hybridization, the DNA chips were washed twice in 2 × SSC containing 0.2% SDS at 50°C for 20 min followed by washing in 2 × SSC at 50°C for 10 min, and then hybridization signals were examined and analyzed by means of a DNA chip reader adopting multi-beam excitation technology according to the manufacturer's instructions (Yokogawa Electric Corporation).

Results and discussion

Different cells have different levels of gene silencing mediated by endogenous *let-7*

In order to examine the effects of endogenous miRNAs on the expression of their target genes, we chose the *let-7* miRNA since it had been studied well and because it appeared to be expressed ubiquitously. To investigate the effects of endogenous *let-7* on the expression of its target genes, we performed widely-used assay with luciferase reporter genes carrying target sequences for miRNAs, by which gene silencing with mRNA digestion and translation inhibition mediated by miRNAs can be detected [11, 14, 15, 21, 30–34]. In this study, two types of reporter plasmids were constructed: one carries perfectly matched target sequence (PMTS) for *let-7* in the 3′UTR of the *Renilla luciferase* reporter gene to monitor RNAi activity and the other has three bulged binding sites (3 × BBS) for *let-7* to monitor translation-inhibition activity (Fig. 1), according to the previous studies described by Pillai et al. [14] and Schmitter et al. [34], where the target sequences were shown to undergo distinct gene silencing to each other as described above. The reporter plasmids and empty vector (psiCHECK-2 or psiCHECK-2TK) as a control were transfected into various mammalian cells, and expression of the reporter genes was examined. Figure 2 shows the results. When the target reporter gene carrying PMTS was examined, the expression of the reporter gene (carrying PMTS) was strongly inhibited in the cells except F9 cell, suggesting that potent RNAi activity mediated by endogenous *let-7* occurred in the cells. Interestingly, when the

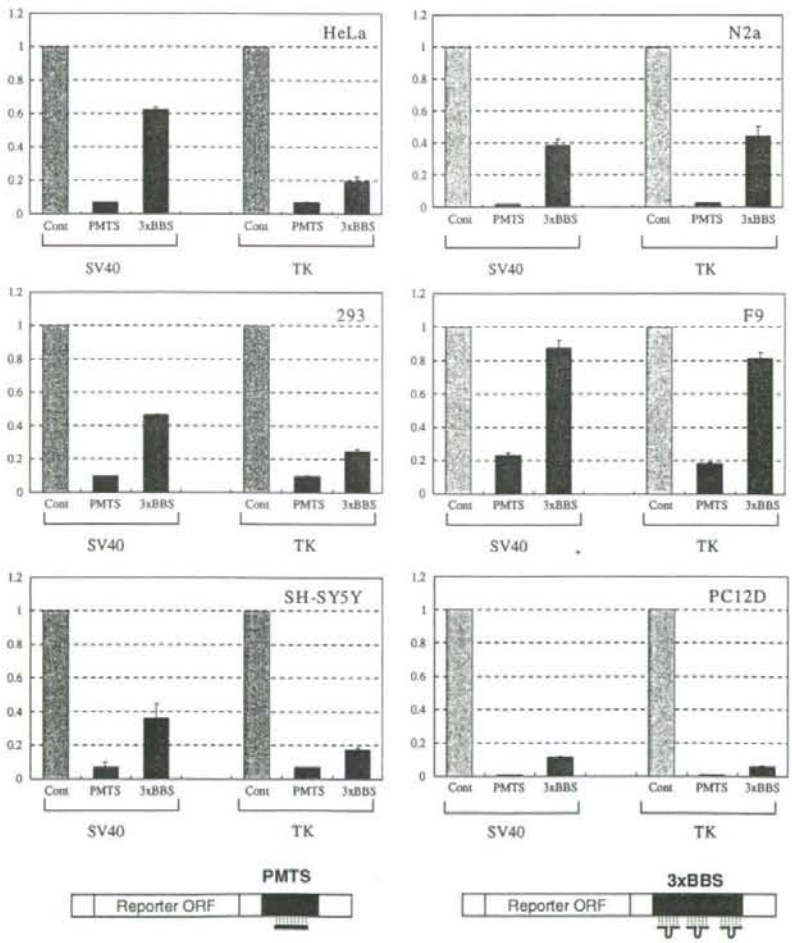

Fig. 2 Knockdown potency of gene silencing mediated by endogenous *let-7*. Reporter genes carrying perfectly matched target sequence (PMTS) and three bulged binding sites (3 × BBS) for *let-7* were constructed (Fig. 1), which are schematically shown together with *let-7* represented by a solid bar or crooked lines. The reporter genes were introduced into indicated cells, and the expression levels of the reporters were examined. Ratios of normalized target (*Renilla*) luciferase activity to control (*Photinus*) luciferase activity are shown: the ratios of luciferase activity in the presence of either PMTS (green bars) or 3 × BBS (pink bars) are normalized to the ratio obtained with the psiCHECK-2 or psiCHECK-2-TK empty plasmid (gray bars) as a control. Data are averages of at least four independent experiments. Error bars represent standard deviations. The SV40 and TK promoters, which drive the reporter genes (Fig. 1), are indicated

reporter gene carrying 3 × BBS was investigated, the level of expression of the target reporter gene varied among the cells, i.e., different cells had different levels of suppression against the target gene. Of the cells investigated, F9 cell exhibited the weakest suppression of the target reporter genes for *let-7*.

Various expression levels of endogenous *let-7* among the cells

In order to address why different cells had different levels of gene silencing (Fig. 2), we investigated the expression of endogenous *let-7* in the cells by means of RT-PCR using specific primers for *let-7a*. As shown in Fig. 3, the results of end-point PCR analyses revealed that the level of *let-7a* varied among the cells: PC12D and SH-SY5Y cells appear to express *let-7a* in a higher level and F9 cell may hardly express it. F9 cell together with N2a cell as a control were further examined by RT-real time PCR followed by analysis with the cycle threshold (Ct) method, and the results suggested that F9 cell might express approximately one-sixth to one-eighth as much *let-7a* as N2a cell (data not shown). We also examined expression profiles of the *let-7* family members by means of the *Genopal*-MICM DNA chips, where DNA probes for the *let-7* members (the mouse *let-7a-g* and *-7i*) are installed. The results of the expression profile analysis indicated that not only *let-7a* but also other *let-7* members were barely present in F9 cell (Fig. 4).

Based on the results, it should be noted that there is a possible correlation between the expression level of *let-7* (Figs. 3, 4) and the suppression level of the target reporter genes (Fig. 2). Data consistent with the possibility were also obtained from experiments with an anti-*let-7* inhibitor: the expression level of the target reporter gene carrying either PMTS or 3 × BBS was increased with an increasing amount of the anti-*let-7* inhibitor, suggesting the reduction of gene silencing mediated by *let-7* with an increasing amount of the anti-*let-7* inhibitor (Fig. 7a). To further

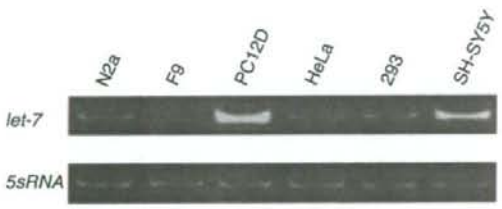

Fig. 3 Expression of endogenous *let-7* in various cells. Total RNA extracted from the indicated cells was subjected to cDNA synthesis, and end-point PCR analysis of *let-7* and *5sRNA* as a control was carried out. The resultant PCR products were examined by electrophoresis with 12% polyacrylamide gels followed by ethidium bromide staining

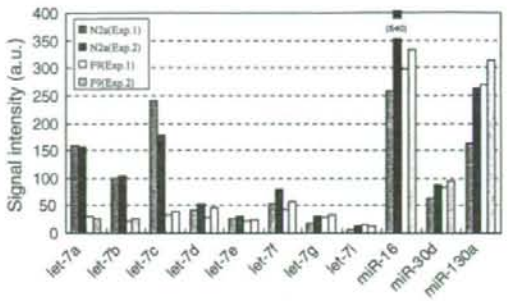

Fig. 4 Expression profiles of *let-7* miRNAs. Small-sized RNAs extracted from F9 and N2a cells were examined by the *Genopal*®-MICM DNA chips (Mitsubishi Rayon). Expression profiles of *let-7* members (indicated) and miR-16, −30d and −130a as positive controls are shown. Hybridization signal intensity of each miRNA was subjected to background subtraction and indicated by arbitrary intensity units (a.u.). The intensity which is over the plotted area is indicated in a parenthesis. Expression profile analysis was repeated individually (Exps. 1 and 2)

evaluate the possibility, we examined the expression of genes associated with RNAi and/or miRNA pathways. The *Ago1-4*, *Dicer*, *Pact*, *Tarbp2*, *Zfp36*, and *Trc6a* genes were investigated by RT-real time PCR (Fig. 5), and the results indicated that the expression profiles of the genes were similar among the cells, suggesting little correlation of the expression of the genes with various suppression levels of the target reporter genes.

Since F9 cell exhibited weak suppression against the target reporter genes for *let-7* (Fig. 2), we examined whether the cell possessed immature gene silencing machinery

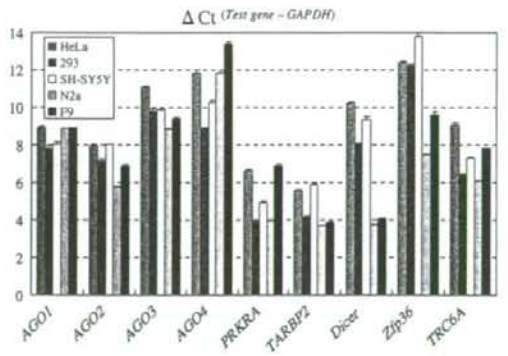

Fig. 5 Expression profiles of genes involved in gene silencing pathways. Total RNA was extracted from indicated cells and examined by RT-real time PCR. The genes examined are indicated. Expression levels of the genes were analyzed by the cycle threshold (Ct) method: the difference between their Ct and the Ct of the *Gapdh* gene examined as a control [$\Delta Ct^{(\text{Test gene} - \text{Gapdh})}$] was calculated and plotted. Data are averages of three measurements by RT-real time PCR analyses. Error bars represent standard deviations

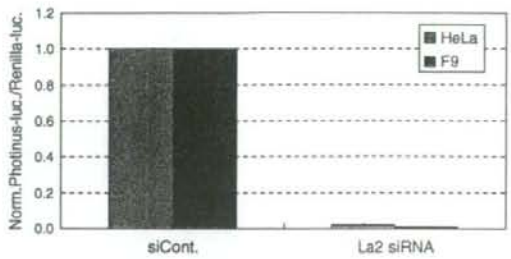

Fig. 6 RNAi activities induced by synthetic siRNA duplex in F9 cells. Chemically synthesized La2 siRNA duplex against the *Photinus luciferase* gene [35] together with pGL3-control (Promega) and phRL-TK plasmids (Promega) carrying *Photinus* and *Renilla luciferase* reporter genes, respectively, were cotransfected into F9 and HeLa (control) cells. Twenty-four hours after transfection, cell lysate was prepared, and dual-luciferase assay was carried out and analyzed as described previously [35]. Data are averages of at least three independent experiments. Error bars represent standard deviations

by using an exogenous (chemically synthesized) siRNA duplex triggering strong RNAi. The La2 siRNA duplex, which can induce strong RNAi activity against the *Photinus luciferase* gene [35], was cotransfected with the target reporter gene into F9 cells. As shown in Fig. 6, consistent with the previous results [35, 36], the cells exhibited potent RNAi, suggesting that F9 cell possesses a full-RNAi machinery. This has been also supported by experiments with a synthetic pre-*let-7* precursor: the expression level of the target reporter gene carrying either PMTS or 3 × BBS was decreased in the presence of the pre-*let-7* precursor (Fig. 7b). Taken together, the data presented here suggest that the expression level of *let-7* greatly influences the level of gene silencing against its target genes.

Effect of transcriptional activity of target gene on gene silencing

In this study, we also examined the effect of transcriptional activity of the target reporter genes on gene silencing. The SV40 and TK promoters, which drive the reporter genes (Fig. 1), appear to have different promoter activities: the transcriptional activity of the SV40 promoter appears to be stronger than that of the TK promoter in the cells examined here (Fig. 8). When suppression level was examined between the promoters, little or no difference in suppression of the reporter gene carrying PMTS was detected, and in contrast, the reporter gene carrying 3 × BBS appeared to exhibit difference in suppression level between the promoters. Table 3 shows relative expression level of the target reporter gene carrying 3 × BBS, when the expression level of the target gene carrying PMTS is given as 1; and the data indicate differences in the relative expression levels between the promoters. Taken together, it is suggested that

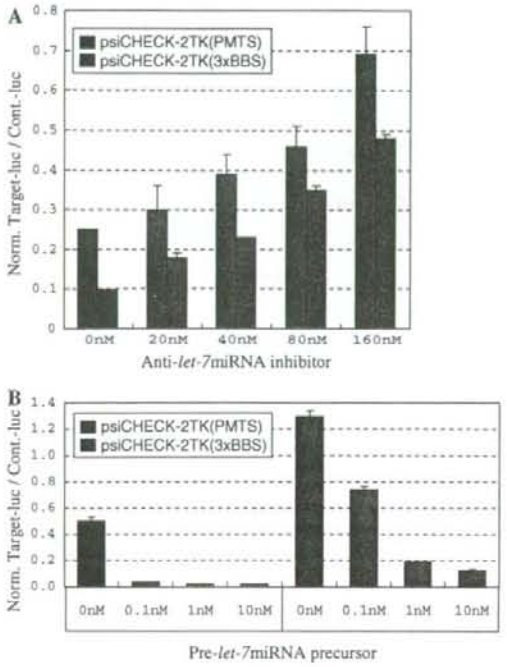

Fig. 7 Dose-dependent suppression of target reporter genes. The psiCHECK-2-TK(PMTS) and psiCHECK-2-TK(3 × BBS) plasmids were cotransfected with an increasing amount of the Anti-miR miRNA inhibitor of *let-7a* (Ambion), from 0 to 160 nM, into 293 cells (**a**), or an increasing amount of the Pre-miR miRNA precursor of *let-7a* (Ambion), from 0 to 20 nM, into F9 cells (**b**). 48 and 24 h after transfection with the inhibitor and precursor, respectively, cell extract was prepared and dual-luciferase assay was carried out. Data are presented as normalized ratios of target (*Renilla*) luciferase activity to control (*Photinus*) luciferase activity as in Fig. 2

different expression levels of one particular target gene undergoing gene silencing by translation inhibition may be reflected in a variety of its gene expression, whereas those undergoing gene silencing by RNAi may be not.

Variety of gene silencing

The data presented here suggest possible parameters conferring a variety of gene silencing: (i) level of endogenous miRNA and (ii) level of target mRNA. In addition, it has been known that various base-pairing interactions can be formed between miRNAs and their target mRNAs [31, 37]. It is conceivable that these parameters presumably raise a great deal of combination between miRNAs and target mRNAs in a qualitative and quantitative manner. Accordingly, the resultant gene silencing based on such a combination may yield various levels of suppression against target mRNAs, thereby conferring a variety of gene expression.

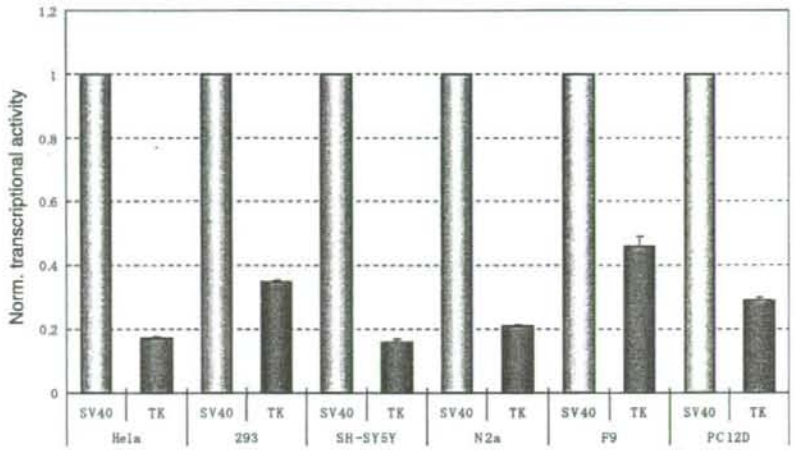

Fig. 8 Transcriptional activity. The transcriptional activities of the SV40 and TK promoters which drive the target reporter (*Renilla luciferase*) gene were investigated in the cells (indicated). The psiCHECK-2 and psiCHECK-2-TK empty plasmids were introduced into the cells and the expressed luciferases were examined as in Fig. 2. Ratios of normalized *Renilla* luciferase activity to control *Photinus* luciferase activity are shown: the ratio of the *Renilla* luciferase activity in the presence of psiCHECK-2-TK is normalized to the ratio obtained in the presence of psiCHECK-2 in each cell. Data are averages of at least three independent experiments. Error bars represent standard deviations

Table 3 Relative expression levels of target reporter gene carrying 3 × BBS

Cell name	SV40[a]	TK[a]
HeLa	9.09	2.85
293	4.84	2.53
SH-SY5Y	5.12	2.57
N2a	21.7	16.3
F9	3.76	4.44
PC12D	11.4	6.1

The relative expression level is indicated when the expression level of the target reporter gene carrying PMTS is given as 1 under each promoter

[a] Used promoters for driving the target reporter genes

Acknowledgements We would like to thank T. Fukushima (Mitsubishi Rayon) for his helpful assistance. This work was supported in part by research grants from the Ministry of Health, Labour and Welfare of Japan and by Grants-in-Aid for Scientific Research from the Japan Society for the Promotion of Science.

References

1. Lee Y, Ahn C, Han J et al (2003) The nuclear RNase III Drosha initiates microRNA processing. Nature 425:415–419. doi:10.1038/nature01957
2. Denli AM, Tops BB, Plasterk RH et al (2004) Processing of primary microRNAs by the Microprocessor complex. Nature 432:231–235. doi:10.1038/nature03049
3. Bartel DP (2004) MicroRNAs: genomics, biogenesis, mechanism, and function. Cell 116:281–297. doi:10.1016/S0092-8674(04)00045-5
4. Krichevsky AM, King KS, Donahue CP et al (2003) A microRNA array reveals extensive regulation of microRNAs during brain development. RNA 9:1274–1281. doi:10.1261/rna.5980303
5. Lagos-Quintana M, Rauhut R, Yalcin A et al (2002) Identification of tissue-specific microRNAs from mouse. Curr Biol 12:735–739. doi:10.1016/S0960-9822(02)00809-6
6. Babak T, Zhang W, Morris Q et al (2004) Probing microRNAs with microarrays: tissue specificity and functional inference. RNA 10:1813–1819. doi:10.1261/rna.7119904
7. Liu CG, Calin GA, Meloon B et al (2004) An oligonucleotide microchip for genome-wide microRNA profiling in human and mouse tissues. Proc Natl Acad Sci USA 101:9740–9744. doi:10.1073/pnas.0403293101
8. Hutvagner G, Zamore PD (2002) A microRNA in a multiple-turnover RNAi enzyme complex. Science 297:2056–2060. doi:10.1126/science.1073827
9. Caudy AA, Myers M, Hannon GJ et al (2002) Fragile X-related protein and VIG associate with the RNA interference machinery. Genes Dev 16:2491–2496. doi:10.1101/gad.1025202
10. Schwarz DS, Hutvagner G, Du T et al (2003) Asymmetry in the assembly of the RNAi enzyme complex. Cell 115:199–208. doi:10.1016/S0092-8674(03)00759-1
11. Zeng Y, Yi R, Cullen BR (2003) MicroRNAs and small interfering RNAs can inhibit mRNA expression by similar mechanisms. Proc Natl Acad Sci USA 100:9779–9784. doi:10.1073/pnas.1630797100
12. Olsen PH, Ambros V (1999) The lin-4 regulatory RNA controls developmental timing in Caenorhabditis elegans by blocking LIN-14 protein synthesis after the initiation of translation. Dev Biol 216:671–680. doi:10.1006/dbio.1999.9523
13. Liu J, Valencia-Sanchez MA, Hannon GJ et al (2005) MicroRNA-dependent localization of targeted mRNAs to mammalian P-bodies. Nat Cell Biol 7:719–723. doi:10.1038/ncb1274
14. Pillai RS, Bhattacharyya SN, Artus CG et al (2005) Inhibition of translational initiation by Let-7 MicroRNA in human cells. Science 309:1573–1576. doi:10.1126/science.1115079

15. Doench JG, Petersen CP, Sharp PA (2003) siRNAs can function as miRNAs. Genes Dev 17:438–442. doi:10.1101/gad.1064703
16. Yekta S, Shih IH, Bartel DP (2004) MicroRNA-directed cleavage of HOXB8 mRNA. Science 304:594–596. doi:10.1126/science.1097434
17. Chen CZ, Li L, Lodish HF et al (2004) MicroRNAs modulate hematopoietic lineage differentiation. Science 303:83–86. doi:10.1126/science.1091903
18. Chen JF, Mandel EM, Thomson JM et al (2006) The role of microRNA-1 and microRNA-133 in skeletal muscle proliferation and differentiation. Nat Genet 38:228–233. doi:10.1038/ng1725
19. Schratt GM, Tuebing F, Nigh EA et al (2006) A brain-specific microRNA regulates dendritic spine development. Nature 439:283–289. doi:10.1038/nature04367
20. Zhao Y, Samal E, Srivastava D (2005) Serum response factor regulates a muscle-specific microRNA that targets Hand2 during cardiogenesis. Nature 436:214–220. doi:10.1038/nature03817
21. Cheng AM, Byrom MW, Shelton J et al (2005) Antisense inhibition of human miRNAs and indications for an involvement of miRNA in cell growth and apoptosis. Nucleic Acids Res 33:1290–1297. doi:10.1093/nar/gki200
22. Hornstein E, Mansfield JH, Yekta S et al (2005) The microRNA miR-196 acts upstream of Hoxb8 and Shh in limb development. Nature 438:671–674. doi:10.1038/nature04138
23. Calin GA, Dumitru CD, Shimizu M et al (2002) Frequent deletions and down-regulation of micro-RNA genes miR15 and miR16 at 13q14 in chronic lymphocytic leukemia. Proc Natl Acad Sci USA 99:15524–15529. doi:10.1073/pnas.242606799
24. Eis PS, Tam W, Sun L et al (2005) Accumulation of miR-155 and BIC RNA in human B cell lymphomas. Proc Natl Acad Sci USA 102:3627–3632. doi:10.1073/pnas.0500613102
25. He L, Thomson JM, Hemann MT et al (2005) A microRNA polycistron as a potential human oncogene. Nature 435:828–833. doi:10.1038/nature03552
26. Johnson SM, Grosshans H, Shingara J et al (2005) RAS is regulated by the let-7 microRNA family. Cell 120:635–647. doi:10.1016/j.cell.2005.01.014
27. Hohjoh H, Fukushima T (2007) Marked change in microRNA expression during neuronal differentiation of human teratocarcinoma NTera2D1 and mouse embryonal carcinoma P19 cells. Biochem Biophys Res Commun 362:360–367. doi:10.1016/j.bbrc.2007.07.189
28. Ohnishi Y, Tokunaga K, Kaneko K, Hohjoh H (2006) Assessment of allele-specific gene silencing by RNA interference with mutant and wild-type reporter alleles. J RNAi Gene Silencing 2:154–160
29. Hohjoh H, Fukushima T (2007) Expression profile analysis of microRNA (miRNA) in mouse central nervous system using a new miRNA detection system that examines hybridization signals at every step of washing. Gene 391:39–44. doi:10.1016/j.gene.2006.11.018
30. Kiriakidou M, Nelson PT, Kouranov A et al (2004) A combined computational-experimental approach predicts human microRNA targets. Genes Dev 18:1165–1178. doi:10.1101/gad.1184704
31. Lewis BP, Shih IH, Jones-Rhoades MW et al (2003) Prediction of mammalian microRNA targets. Cell 115:787–798. doi:10.1016/S0092-8674(03)01018-3
32. O'Donnell KA, Wentzel EA, Zeller KI et al (2005) c-Myc-regulated microRNAs modulate E2F1 expression. Nature 435:839–843. doi:10.1038/nature03677
33. Petersen CP, Bordeleau ME, Pelletier J et al (2006) Short RNAs repress translation after initiation in mammalian cells. Mol Cell 21:533–542. doi:10.1016/j.molcel.2006.01.031
34. Schmitter D, Filkowski J, Sewer A et al (2006) Effects of Dicer and Argonaute down-regulation on mRNA levels in human HEK293 cells. Nucleic Acids Res 34:4801–4815. doi:10.1093/nar/gkl646
35. Hohjoh H (2002) RNA interference (RNAi) induction with various types of synthetic oligonucleotide duplexes in cultured human cells. FEBS Lett 521:195–199. doi:10.1016/S0014-5793(02)02860-0
36. Sago N, Omi K, Tamura Y et al (2004) RNAi induction and activation in mammalian muscle cells where Dicer and eIF2C translation initiation factors are barely expressed. Biochem Biophys Res Commun 319:50–57. doi:10.1016/j.bbrc.2004.04.151
37. Lewis BP, Burge CB, Bartel DP (2005) Conserved seed pairing, often flanked by adenosines, indicates that thousands of human genes are microRNA targets. Cell 120:15–20. doi:10.1016/j.cell.2004.12.035

THE JOURNAL OF BIOLOGICAL CHEMISTRY VOL. 283, NO. 35, pp. 23731–23738, August 29, 2008

Aberrant Interaction between Parkinson Disease-associated Mutant UCH-L1 and the Lysosomal Receptor for Chaperone-mediated Autophagy*[S]

Received for publication, March 10, 2008, and in revised form, June 12, 2008 Published, JBC Papers in Press, June 12, 2008, DOI 10.1074/jbc.M801918200

Tomohiro Kabuta[‡1], Akiko Furuta[‡], Shunsuke Aoki[‡2], Koh Furuta[§], and Keiji Wada[‡3]

From the [‡]Department of Degenerative Neurological Diseases, National Institute of Neuroscience, National Center of Neurology and Psychiatry, 4-1-1 Ogawahigashi, Kodaira, Tokyo 187-8502, Japan and the [§]Division of Clinical Laboratories, National Cancer Center Hospital, 5-1-1 Tsukiji, Chuo-ku, Tokyo 104-0045, Japan

Parkinson disease (PD) is the most common neurodegenerative movement disorder. An increase in the amount of α-synuclein protein could constitute a cause of PD. α-Synuclein is degraded at least partly by chaperone-mediated autophagy (CMA). The I93M mutation in ubiquitin C-terminal hydrolase L1 (UCH-L1) is associated with familial PD. However, the relationship between α-synuclein and UCH-L1 in the pathogenesis of PD has remained largely unclear. In this study, we found that UCH-L1 physically interacts with LAMP-2A, the lysosomal receptor for CMA, and Hsc70 and Hsp90, which can function as components of the CMA pathway. These interactions were abnormally enhanced by the I93M mutation and were independent of the monoubiquitin binding of UCH-L1. In a cell-free system, UCH-L1 directly interacted with the cytosolic region of LAMP-2A. Expression of I93M UCH-L1 in cells induced the CMA inhibition-associated increase in the amount of α-synuclein. Our findings may provide novel insights into the molecular links between α-synuclein and UCH-L1 and suggest that aberrant interaction of mutant UCH-L1 with CMA machinery, at least partly, underlies the pathogenesis of PD associated with I93M UCH-L1.

Parkinson disease (PD)[4] is the most common neurodegenerative movement disorder characterized by progressive degeneration confined mostly to dopaminergic neurons in the substantia nigra pars compacta. Although the majority of PD cases occur sporadically, nine genes have been reported to be associated with familial forms of PD. Several missense mutations in the α-synuclein gene are linked to dominantly inherited PD (1–3). Duplication and triplication of the α-synuclein gene were also shown to cause familial PD or parkinsonism (4–6), indicating that increases in the levels of α-synuclein could constitute a cause of PD. α-Synuclein is a major component of cytoplasmic inclusions called Lewy bodies in the brains of patients with sporadic PD (7, 8). These findings raised the idea that α-synuclein plays a central role in the pathogenesis of PD. Therefore, elucidating the molecular relationships between α-synuclein and other familial PD-associated proteins is important for understanding the mechanisms that underlie the pathology of PD.

A missense mutation in the ubiquitin C-terminal hydrolase L1 (UCH-L1) gene, leading to an I93M substitution at the protein level, has been reported in two affected siblings of a German family with dominantly inherited PD (9). In this family, four of seven family members were affected with PD. However, the family members, except the two siblings, were not genotyped. There was an unaffected presumed carrier of the I93M mutation in the family. Therefore, the link between the I93M mutation and the development of PD has been questioned (10, 11). To clarify the link between the mutation and PD, we have generated UCH-L1^{I93M} transgenic mice and reported that these mice exhibit progressive dopaminergic cell loss (12). In addition, we have shown that, compared with UCH-L1^{WT}, UCH-L1^{I93M} exhibits increased insolubility and levels of interactions with other proteins in mammalian cells, features that are characteristic of several neurodegenerative disease-linked mutants (13). These findings suggest that the I93M mutation in UCH-L1 contributes to the pathogenesis of PD. UCH-L1 has also been identified as a component of several inclusion bodies characteristic of neurodegenerative diseases including Lewy bodies (14). A polymorphism in the UCH-L1 gene, resulting in an S18Y substitution at the amino acid residue level, has been reported to be associated with decreased risk of PD in certain populations but not in other populations (15, 16). We have also reported that UCH-L1^{I93M} and carbonyl-modified UCH-L1, which is associated with sporadic PD (17), display shared aberrant properties (13), suggesting that carbonyl-modified UCH-L1 constitutes one of the causes of sporadic PD.

* This work was supported by grants-in-aid for scientific research from the Japan Society for the Promotion of Science; a research grant in priority area research from the Ministry of Education, Culture, Sports, Science, and Technology, Japan; grants-in-aid for scientific research from the Ministry of Health, Labor, and Welfare, Japan; and the Program for Promotion of Fundamental Studies in Health Sciences of the National Institute of Biomedical Innovation and the New Energy and Industrial Technology Development Organization, Japan. The costs of publication of this article were defrayed in part by the payment of page charges. This article must therefore be hereby marked "*advertisement*" in accordance with 18 U.S.C. Section 1734 solely to indicate this fact.

[S] The on-line version of this article (available at http://www.jbc.org) contains supplemental "Experimental Procedures," Figs. S1 and S2, and an additional reference.

[1] To whom correspondence may be addressed. Tel.: 81-42-346-1715; Fax: 81-42-346-1745; E-mail: kabuta@ncnp.go.jp.

[2] Present address: Dept. of Bioscience and Bioinformatics, Kyushu Inst. of Technology, 680-4 Kawazu, Iizuka-shi, Fukuoka 820-8502, Japan.

[3] To whom correspondence may be addressed. Tel.: 81-42-346-1715; Fax: 81-42-346-1745; E-mail: wada@ncnp.go.jp.

[4] The abbreviations used are: PD, Parkinson disease; UCH-L1, ubiquitin C-terminal hydrolase L1; WT, wild-type; CMA, chaperone-mediated autophagy; LAMP-2, lysosome-associated membrane protein type 2; Hsc70, heat shock cognate protein 70; Hsp90, heat shock protein 90; GAPDH, glyceraldehyde-3-phosphate dehydrogenase.

UCH-L1 is one of the most abundant proteins in the brain (1–5% of total soluble protein) (18) and is thought to hydrolyze ubiquitin conjugates into monoubiquitin (19). UCH-L1 was also reported to function as a ubiquitin ligase for monoubiquitinated α-synuclein in a cell-free system (20). Other than these enzymatic activities, we have reported that UCH-L1 stabilizes monoubiquitin by binding to monoubiquitin in neurons (21). Although the hydrolase activity of UCH-L1^{I93M} and the binding of UCH-L1^{I93M} to monoubiquitin are decreased compared with those of UCH-L1^{WT} (9, 13, 22), we have shown that mice deficient in UCH-L1 do not display obvious dopaminergic cell loss (21, 23). These observations indicate that the main cause of UCH-L1^{I93M}-associated PD may not be a loss of UCH-L1 function but an acquired toxicity of UCH-L1^{I93M}. Our previous studies also suggest that aberrantly enhanced physical interactions between UCH-L1^{I93M} and multiple proteins, including tubulin, underlie the toxic functions of UCH-L1^{I93M} (13).

However, the molecular relationship between α-synuclein and UCH-L1 in the pathogenesis of PD has remained largely unclear. α-Synuclein is known to be degraded at least partly by chaperone-mediated autophagy (CMA) (24), in which substrate proteins are selectively transported to and degraded in lysosomes (25). In this study, we sought to identify novel UCH-L1-interacting proteins. We found that UCH-L1 physically interacts with lysosome-associated membrane protein type 2A (LAMP-2A), heat shock cognate protein 70 (Hsc70), and heat shock protein 90 (Hsp90), all of which are components of the CMA pathway (26). These interactions were enhanced by the I93M mutation in UCH-L1 and were independent of the interaction between monoubiquitin and UCH-L1. We also provide the data suggesting that the aberrant interaction of UCH-L1 with CMA machinery results in the accumulation of α-synuclein.

EXPERIMENTAL PROCEDURES

Plasmids—pCI-neo-hUCH-L1 plasmids containing human WT UCH-L1 and UCH-L1 variants with or without a FLAG tag were prepared as described previously (13). The regulatory expression plasmids pTRE-Tight-hUCH-L1 containing WT and I93M UCH-L1 with a FLAG tag at the C terminus of UCH-L1 were constructed by ligating the cDNA encoding UCH-L1 into the pTRE-Tight (Clontech) vector. The expression plasmid pCI-neo-hα-synuclein was constructed using the pCI-neo mammalian expression vector (Promega), and the expression plasmid pCI-neo-ΔDQ α-synuclein was generated using a QuikChange site-directed mutagenesis kit (Stratagene).

Cell Culture and Transfection—COS-7 cells were maintained in Dulbecco's modified Eagle's medium (Sigma) supplemented with 10% fetal bovine serum (JRH Biosciences, Lenexa, KS). IMR-90 cells, which have been used to study CMA (27), were cultured as described in the literature (27). NIH-3T3 cells stably expressing human UCH-L1 with a FLAG-hemagglutinin double tag at the N terminus were cultured as described previously (13). Transient transfection of COS-7 and IMR-90 cells with each vector was performed using Lipofectamine reagent (Invitrogen) and Lipofectamine LTX reagent (Invitrogen), respectively. There was no notable difference in the transfection efficiency among the culture dishes (wells) in our experimental conditions (data not shown).

Immunoblotting and Immunoprecipitation—Preparation of the detergent (1% Triton X-100)-soluble fraction was performed as described previously (28). The cytosolic fraction that does not contain LAMP-2, a marker of lysosomes, and the crude lysosomal fraction containing LAMP-2 (supplemental Fig. S1*A*) were prepared according to the method described by Pertoft *et al.* (29). SDS-PAGE was performed under reducing conditions. Immunoblotting was performed according to standard procedures as described previously (30). For some experiments, Can Get Signal Immunoreaction Enhancer Solution (Toyobo, Osaka, Japan) was used. The signal intensity was quantified by densitometry using FluorChem software (Alpha Innotech, San Leandro, CA). Immunoprecipitation was performed using anti-FLAG M2 affinity gel (Sigma) or 10 μg/ml antibodies (unless otherwise mentioned) with protein G-Sepharose (GE Healthcare), as described previously (13). The antibodies used were as follows. Antibodies against UCH-L1, Cu,Zn-superoxide dismutase 1, Hsc70, and Hsp90 were purchased from Ultra-Clone, Stressgen Bioreagents (Victoria, Canada), Affinity BioReagents (Golden, CO), and BD Transduction Laboratories (Franklin Lakes, NJ), respectively. Anti-β-actin, Mcl-1, and FLAG antibodies were from Sigma. Antibodies against α-synuclein and glyceraldehyde-3-phosphate dehydrogenase (GAPDH) were from Chemicon (Temecula, CA). Anti-p53 and Bcl-xL antibodies were from Cell Signaling. Anti-Bcl-2, Ubc9, NF-κB p65, and LAMP-2 antibodies were from Santa Cruz Biotechnology. The rabbit polyclonal anti-LAMP-2A antibody was raised in rabbit against a synthetic peptide (CYFIGLKHHHAGYEQF) containing an amino acid sequence corresponding to the cytosolic region of human LAMP-2A. The specificity of the anti-LAMP-2A antibody was confirmed as shown in supplemental Fig. S1, *B* and *C*.

Pulldown Assay—Recombinant human UCH-L1 proteins without a tag were prepared as described previously (13). A pulldown assay was performed as described previously (13) with slight modifications. Streptavidin-Sepharose (GE Healthcare) was blocked with 3% bovine serum albumin for 15 h to prevent nonspecific binding of UCH-L1 to the beads and washed three times with phosphate-buffered saline containing 0.05% Triton X-100. Ten μg of UCH-L1 (wild-type or I93M) and 2 nmol of synthetic peptides conjugated to biotin (control or LAMP-2A peptide, Invitrogen) were mixed and incubated for 15 h in phosphate-buffered saline containing 0.05% Triton X-100. Twenty μl of streptavidin beads blocked with bovine serum albumin was then added, and incubation was continued for 1 h. After beads were washed three times with phosphate-buffered saline containing 0.05% Triton X-100, proteins were eluted with SDS sample buffer and subjected to SDS-PAGE.

UCH-L1 Degradation Assay—COS-7 cells were cotransfected with pTet-Off and pTRE-Tight-hUCH-L1. Twenty-four h after transfection, transcription of UCH-L1-FLAG gene was suppressed by adding 100 ng/ml doxycycline and incubating for 4 h. Then, cells were harvested at the 0-, 24-, and 48-h time

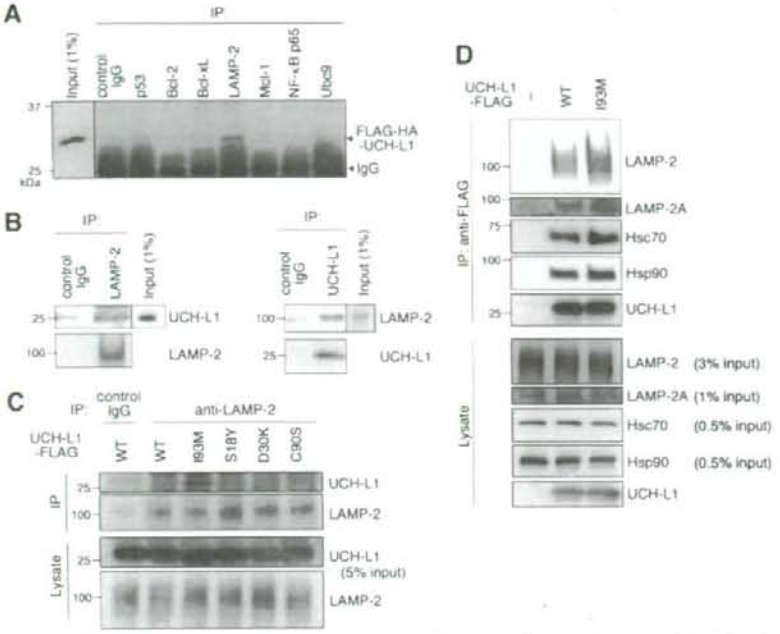

FIGURE 1. **Physical interactions of UCH-L1 with LAMP-2A, Hsc70, and Hsp90.** *A*, lysates of NIH-3T3 cells stably expressing FLAG-hemagglutinin (*HA*)-tagged UCH-L1 were immunoprecipitated (*IP*) with antibodies against cell death- or protein degradation-related proteins and analyzed by immunoblotting using anti-UCH-L1 antibody. A representative blot including immunoprecipitant with anti-LAMP-2 antibody is shown. *B*, mouse (C57BL/6J) whole brain lysates were immunoprecipitated with control IgG, anti-LAMP-2, or anti-UCH-L1 antibody and immunoblotted with anti-UCH-L1 and LAMP-2 antibodies. *C*, lysates of COS-7 cells transfected with the indicated constructs were immunoprecipitated with 5 μg/ml control IgG or anti-LAMP-2 antibody and analyzed by immunoblotting using anti-UCH-L1 antibody. *D*, lysates of COS-7 cells transfected with the indicated constructs (−, empty vector) were immunoprecipitated with anti-FLAG beads and immunoblotted using anti-LAMP2, LAMP-2A, Hsc70, Hsp90, and UCH-L1 antibodies.

points after the suppression of the gene and analyzed by immunoblotting. Pulse-chase analyses were performed as described previously (21) with some modifications. COS-7 cells transfected with pCI-neo-hUCH-L1-FLAG were washed and incubated with methionine-, cysteine-, and cystine-free medium for 1 h. The cells were pulsed with 0.1 mCi/ml [^{35}S]Met and [^{35}S]Cys (Expre^{35}S^{35}S protein labeling mixture, PerkinElmer Life Sciences) for 1 h and then washed and chased with 3 mM methionine and cysteine for 48 h. At the 0-, 24-, and 48-h time points, the cells were harvested for immunoprecipitation with anti-FLAG M2 affinity gel. Following SDS-PAGE on a 15% gel, radioactive bands were detected and analyzed by using a BAS-5000 imaging analyzer (Fujifilm, Tokyo, Japan).

Statistical Analysis—For comparison of two groups, the statistical significance of differences was determined by the Student's *t* test.

RESULTS

UCH-L1 Interacts with LAMP-2A, Hsc70, and Hsp90—We have previously shown that soluble UCH-L1 interacts with multiple proteins in mammalian cells and that one of the UCH-L1-interacting proteins is α/β-tubulin (13). In this study, we further screened for UCH-L1-interacting proteins using a coimmunoprecipitation assay (Fig. 1*A*). We identified LAMP-2 as a novel UCH-L1-interacting protein (Fig. 1*A*). To confirm this interaction *in vivo*, a coimmunoprecipitation assay was performed using mouse whole brain lysate. Interaction between endogenous UCH-L1 and endogenous LAMP-2 was observed (Fig. 1*B*). LAMP-2 exists in three different isoforms, LAMP-2A, LAMP-2B, and LAMP-2C, which are produced by the alternative splicing of the LAMP-2 pre-mRNA (31). LAMP-2A forms a complex with chaperones such as Hsc70 and Hsp90 and functions as a receptor for CMA at the lysosomal membrane (26). Because α-synuclein has been reported to interact with LAMP-2A (24), we tested for interactions between UCH-L1 and LAMP-2A, Hsc70, and Hsp90. The UCH-L1 immunoprecipitant included LAMP-2A as well as Hsc70 and Hsp90 (Fig. 1*D*). These results indicate that UCH-L1 interacts with LAMP-2A, Hsc70, and Hsp90 in mammalian cells.

UCH-L1 Can Be Degraded by Macroautophagy—Although UCH-L1 physically interacts with LAMP-2A, UCH-L1 is not a presumable substrate for CMA because UCH-L1 does not contain a KFERQ-like motif, which is required for substrate proteins to be degraded by CMA (32). Therefore, we speculated that UCH-L1 is degraded by other degradation pathways in mammalian cells. We used a regulatory protein expression system to switch off the expression of UCH-L1 by adding doxycycline, to follow UCH-L1 degradation. Degradation of UCH-L1 was observed 24 or 48 h after expression was switched off, compared with the time point at which expression was switched off (Fig. 2*A*). The half-life of UCH-L1 was >48 h (Fig. 2*A*). Long-lived proteins are known to be mainly degraded by macroautophagy (33). We therefore investigated whether UCH-L1 was degraded by macroautophagy using 3-MA, an inhibitor of macroautophagy (24, 28, 34). The 3-MA treatment significantly inhibited the degradation of UCH-L1 (Fig. 2*A*). Similar results were obtained when we used UCH-L1^{I93M} (Fig. 2*B*). Pulse-chase experiments also showed that the degradations of UCH-L1^{WT} and UCH-L1^{I93M} were significantly inhibited by 3-MA treatment (Fig. 2, *C* and *D*). These results suggest that macroautophagy is one of the major pathways that degrade UCH-L1 in our cell model.

The Interactions of UCH-L1 with LAMP-2A, Hsc70, and Hsp90 Are Enhanced by the I93M Mutation in UCH-L1 and Are Independent of the Interaction between Monoubiquitin and

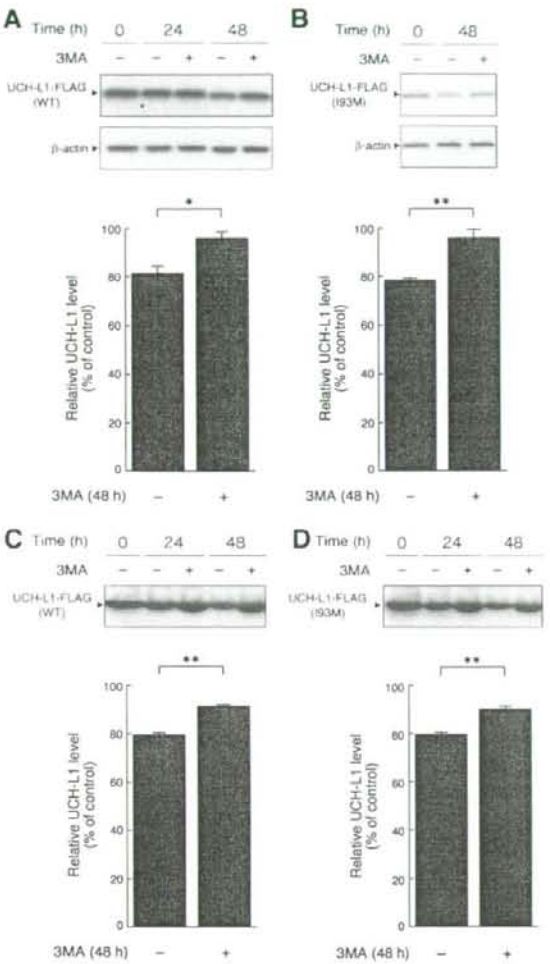

FIGURE 2. **Degradation of UCH-L1 by macroautophagy.** *A* and *B*, COS-7 cells were transfected with pTet-Off and pTRE-Tight-hUCH-L1^{WT} (*A*) or pTRE-Tight-hUCH-L1^{I93M} (*B*). Twenty-four h after transfection, transcription of UCH-L1-FLAG gene was suppressed by adding 100 ng/ml doxycycline and incubating for 4 h. Then, 3-MA (+) or vehicle (−) was added, and cells were harvested at the indicated times after the suppression of the gene and analyzed by immunoblotting (*upper panels*). The relative levels of UCH-L1-FLAG at 48 h after the suppression (% of 0-h control) were quantified by densitometry. Mean values are shown with S.E. (*A*, $n = 4$; *B*, $n = 3$). *, $p < 0.05$; **, $p < 0.01$. *C* and *D*, COS-7 cells were transfected with pCI-neo-hUCH-L1^{WT}-FLAG (*C*) or pCI-neo-hUCH-L1^{I93M}-FLAG (*D*). Twenty-four h after transfection, cells were labeled with [^{35}S]Met and [^{35}S]Cys. Autoradiograms of anti-FLAG immunoprecipitates pulse-chased at the indicated times in the absence or presence of 3-MA are shown (*upper panels*). Relative band intensities at 48 h (% of 0-h control) are quantified. Mean values are shown with S.E. ($n = 3$). **, $p < 0.01$.

UCH-L1—We have previously shown that the amount of each protein interacting with UCH-L1^{I93M} is mostly higher than the amount interacting with UCH-L1^{WT} (13). Consistent with this observation, we found that the amount of LAMP-2A, Hsc70, and Hsp90 interacting with UCH-L1^{I93M} is higher than the amount interacting with UCH-L1^{WT} (~1.8-, 1.3-, and 1.3-fold increases, respectively) (Fig. 1, *C* and *D*, and supplemental Fig. S2*A*). The interactions of LAMP-2, Hsc70, or Hsp90 with UCH-L1^{S18Y}, UCH-L1^{D30K}, which lacks hydrolase activity and binding affinity for ubiquitin (21), and UCH-L1^{C90S}, which lacks hydrolase activity but maintains binding affinity for ubiquitin (21), were not notably changed compared with those of UCH-L1^{WT} (Fig. 1*C*, supplemental Fig. S2*A*, and data not shown). These results suggest that the interaction between UCH-L1 and CMA machinery is independent of both UCH-L1-binding affinity for ubiquitin and the hydrolase activity of UCH-L1. To further show that these interactions are independent of monoubiquitin binding to UCH-L1, and to elucidate the amino acid residues of UCH-L1 involved in the interaction with LAMP-2A, Hsc70, and Hsp90, we performed coimmunoprecipitation assays using a series of alanine substitutions (13) of basic and acidic residues located on the surface of UCH-L1 (Fig. 3*A*). The R63A mutant displayed increased levels of interactions with LAMP-2, Hsc70, and Hsp90, whereas other mutations had no notable effect on the interactions (Fig. 3*A*). We further performed alanine-scanning mutagenesis experiments and found that E174A, D176A, and H185A mutants also displayed increased levels of interactions with LAMP-2, Hsc70, and Hsp90 (Fig. 3*B* and data not shown). Glu^{174}, Asp^{176}, and His^{185} are located near Arg^{63} (Fig. 3*C*). The surface region containing Arg^{63} and His^{185} possesses features that are characteristic of a protein-protein interacting site (35). These observations suggest that this surface region, which is distinct from the ubiquitin-binding region (13, 35), is involved in the interactions with LAMP-2, Hsc70, and Hsp90. The R63A, E174A, D176A, or H185A mutation possibly causes partial misfolding, resulting in increased interactions.

UCH-L1 Directly Interacts with the Cytoplasmic Region of LAMP-2A—LAMP-2 is a type 1 membrane protein, consisting of a short cytoplasmic tail (12 amino acids), one transmembrane domain, and a glycosylated luminal domain (31). To test whether UCH-L1 directly interacts with the cytosolic region of LAMP-2A, we prepared purified recombinant wild-type and I93M UCH-L1 proteins, a peptide containing an amino acid sequence corresponding to the C-terminal cytoplasmic tail of LAMP-2A, and a control peptide (Fig. 4*A*). Purified UCH-L1 proteins and the peptides were mixed, and pulldown assays were performed. A direct interaction between wild-type UCH-L1 and the cytosolic region of LAMP-2A was observed (Fig. 4, *B* and *C*). Consistent with the results of the coimmunoprecipitation assay, UCH-L1^{I93M} exhibited an abnormally increased level of interaction with the cytosolic region of LAMP-2A compared with wild-type UCH-L1 (Fig. 4*D*). Because chaperones, including Hsc70, are considered to be required for the interaction of the CMA substrates with LAMP-2A (36), our results may indicate that UCH-L1 interacts with LAMP-2A in a manner different from the interaction between CMA substrates and LAMP-2A.

UCH-L1^{I93M} Causes Accumulation of α-Synuclein—It has been reported that α-synuclein^{WT} is a CMA substrate, but pathogenic mutants A30P and A53T α-synuclein inhibit CMA by tight binding to LAMP-2A (24). Thus, UCH-L1^{I93M}, which exhibits elevated interactions with LAMP-2A, Hsc70, and Hsp90, may also inhibit CMA. To examine this possibility in mammalian cells, we assessed the effects of UCH-L1^{I93M} on the

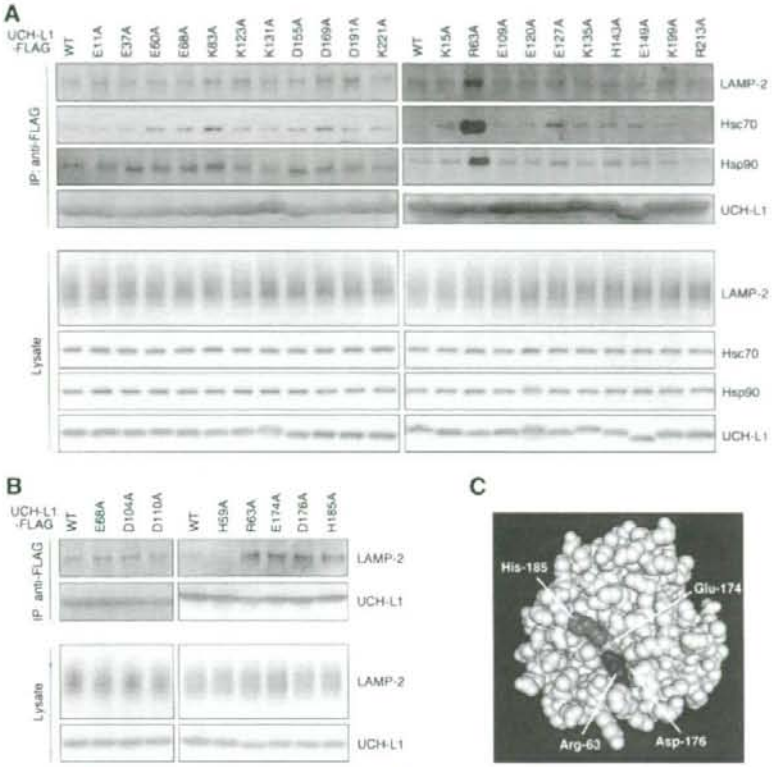

FIGURE 3. **Alanine-scanning mutagenesis of UCH-L1.** *A* and *B*, lysates of COS-7 cells transfected with the indicated constructs were immunoprecipitated (*IP*) with anti-FLAG antibody and analyzed by immunoblotting. *C*, a structural model for human UCH-L1 is shown. Arg^{63}, Glu^{174}, Asp^{176}, and His^{185} are shown in *blue*, *green*, *magenta*, and *red*, respectively, using Cn3D software (version 4.1) and NCBI structural model mmdbId:38174 (35).

protein level of GAPDH, an established substrate of CMA (24), in the lysosomal fraction and whole-cell lysate. The GAPDH level in whole-cell lysate was increased in cells expressing UCH-$L1^{193M}$ compared with that in cells expressing UCH-$L1^{WT}$ (an ~1.5-fold increase) (Fig. 5*A*), whereas the GAPDH level in the lysosomal fraction was decreased in cells expressing UCH-$L1^{193M}$ (an ~2.1-fold decrease) (Fig. 5*B*), supporting the idea that the aberrant interaction of UCH-$L1^{193M}$ with CMA machinery inhibits CMA. The inhibition of CMA also results in the accumulation of other CMA substrates, including α-synuclein (24). We found that the amount of α-$synuclein^{WT}$ was increased in cells expressing UCH-$L1^{193M}$ compared with cells expressing UCH-$L1^{WT}$ (~1.7 and 1.4-fold increases, respectively) (Fig. 5, *C* and *D*) or control mock cells (data not shown). The physical interaction between UCH-L1 and α-synuclein was not detected under these experimental conditions (data not shown). These results suggest that the accumulation of α-synuclein in cells expressing UCH-$L1^{193M}$ is due to the inhibition of CMA-dependent degradation of α-synuclein. α-Synuclein contains a CMA recognition motif, ^{95}VKKDQ^{99}, and mutant α-$synuclein^{\Delta DQ}$, in which ^{98}DQ^{99} is replaced by Ala-Ala, is not degraded by CMA (24). To confirm that the accumulation of α-synuclein in cells expressing UCH-$L1^{193M}$ is associated with CMA-dependent degradation of α-synuclein, we used mutant α-$synuclein^{\Delta DQ}$ and found that the I93M mutation does not affect the α-$synuclein^{\Delta DQ}$ level (~1.0 and 1.0-fold increases, respectively) (Fig. 5, *E* and *F*).

G93A Cu,Zn-superoxide dismutase 1 and WT Cu,Zn-superoxide dismutase 1 are not presumable substrates for CMA because Cu,Zn-superoxide dismutase 1 does not contain a KFERQ-like motif, but they can be degraded by the proteasome and macroautophagy (28). Protein levels of G93A Cu,Zn-superoxide dismutase 1 and WT Cu,Zn-superoxide dismutase 1 in cells transfected with UCH-$L1^{193M}$ were not increased compared with those in cells expressing UCH-$L1^{WT}$ (an ~1.0-fold increase) (Fig. 5*G* and data not shown), suggesting that the I93M mutation does not considerably affect the degradation of proteins by macroautophagy and the proteasome under these experimental conditions.

Contrary to UCH-$L1^{193M}$, UCH-$L1^{D30K}$ and UCH-$L1^{C90S}$ did not increase the amount of α-synuclein in cells (supplemental Fig. S2*B*), indicating that the accumulation of α-synuclein in cells expressing UCH-$L1^{193M}$ is independent of the hydrolase activity of UCH-L1 and the interaction between monoubiquitin and UCH-L1. These observations are consistent with the results showing that the interaction between UCH-L1 and LAMP-2A, Hsc70, or Hsp90 is independent of the enzymatic activity of UCH-L1 and the interaction between monoubiquitin and UCH-L1 (Figs. 1*C* and 3) and also with the idea that the main cause of UCH-$L1^{193M}$-associated PD is not a loss of UCH-L1 function but an acquired toxicity of UCH-$L1^{193M}$.

DISCUSSION

An increase in the amount of α-synuclein protein could constitute a pathogenic factor underlying sporadic PD because the heterozygous duplication of the α-synuclein gene causes familial PD (4, 5), and the deposition of α-synuclein protein is associated with sporadic PD (7, 8, 37). α-$Synuclein^{WT}$ is a CMA substrate, but mutant A30P and A53T α-synuclein inhibit CMA by aberrant tight binding to LAMP-2A (24). Thus, inhibition of CMA by mutant α-synuclein might result in an increase in the amount of α-synuclein protein, leading to the neurodegeneration in familial PD associated with mutant α-synuclein. To date, the relationships between α-synuclein and other familial PD-

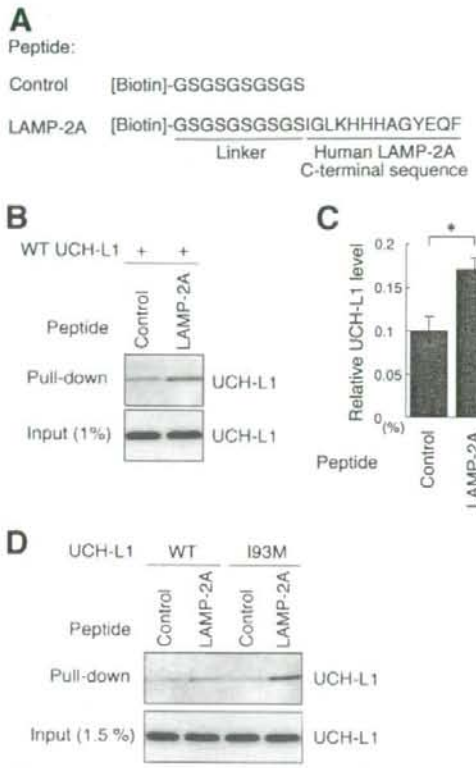

FIGURE 4. **Direct interaction between UCH-L1 and the cytosolic region of LAMP-2A.** *A*, an amino acid sequence of biotin-conjugated peptides is shown. *B* and *C*, 10 μg of recombinant UCH-L1 and 2 nmol of peptides (control or LAMP-2A peptide) were mixed, and a pulldown assay was performed using streptavidin beads. Precipitants were analyzed by immunoblotting (*B*). The levels of UCH-L1 relative to input were quantified by densitometry. Mean values are shown with S.E. ($n = 3$). *, $p < 0.05$. *D*, 10 μg of UCH-L1 (wild-type or I93M) and 2 nmol of peptides (control or LAMP-2A peptide) were mixed, and a pulldown assay was performed.

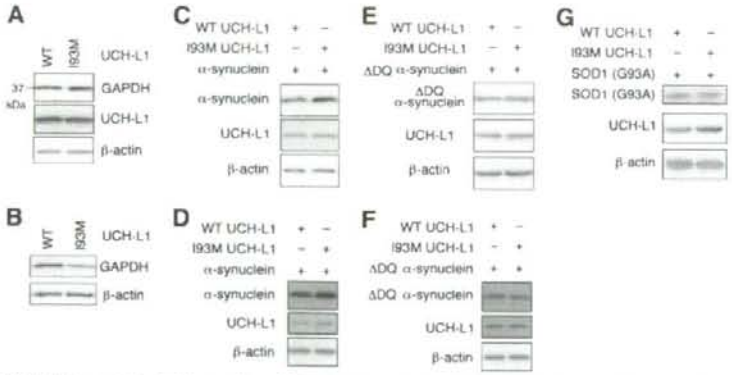

FIGURE 5. **Effects of the I93M mutation of UCH-L1 on CMA and α-synuclein levels.** *A* and *B*, COS-7 cells were transfected with the indicated constructs. Forty-eight h after transfection, whole-cell lysates (*A*) and a lysosomal fraction (*B*) were prepared and analyzed by immunoblotting. *C–G*, COS-7 cells (*C*, *E*, and *G*) or IMR-90 cells (*D* and *F*) were transfected with the indicated constructs. Cell lysates were prepared and analyzed by immunoblotting. Accumulation of α-synuclein^{WT} in cells transfected with UCH-L1^{I93M} was observed in COS-7 (*C*), IMR-90 (*D*), and SH-SY5Y cells (data not shown). The assays were performed at least three times; representative results are shown. *SOD1*, Cu,Zn-superoxide dismutase 1.

associated mutant proteins in the pathogenesis of PD have remained largely unclear. Although it was reported that UCH-L1 polyubiquitinates monoubiquitinated α-synuclein in a cell-free system (20), the relationship between UCH-L1 and non-ubiquitinated α-synuclein in the pathogenesis of PD has also remained unknown.

In the present study, we have shown that familial PD-associated UCH-L1^{I93M} abnormally interacts with LAMP-2A, Hsc70, and Hsp90 and causes an increase in the amounts of α-synuclein and GAPDH, which are CMA substrates, in cultured cells. The increase can be explained by an inhibition of CMA via an aberrant interaction between UCH-L1^{I93M} and CMA machinery because the GAPDH level in the lysosomal fraction was decreased in cells expressing UCH-L1^{I93M} (Fig. 5*B*), and the I93M mutation in UCH-L1 does not affect the levels of α-synuclein$^{\Delta DQ}$, which is not degraded by CMA (Fig. 5, *E* and *F*). These findings suggest that an increase in the amount of α-synuclein protein by inhibition of CMA via the interaction between UCH-L1^{I93M} and CMA machinery underlies one of the causes of familial PD associated with mutant UCH-L1. It is also possible that increases in the amount of other CMA substrates, such as GAPDH, are involved in the pathogenesis of PD. Taken together with a report that pathogenic mutant A30P and A53T α-synuclein exhibit an enhanced interaction with LAMP-2A compared with α-synuclein^{WT} (24), our results indicate that UCH-L1^{I93M} and mutant A30P and A53T α-synuclein share aberrant biochemical properties with respect to their interactions with LAMP-2A. These observations further support the idea that the I93M mutation in UCH-L1 contributes to the pathogenesis of PD.

We revealed that the R63A, E174A, D176A, or H185A substitution in UCH-L1 increases the levels of interactions of UCH-L1 with LAMP-2, Hsc70, and Hsp90 (Fig. 3), suggesting that the surface region containing Arg^{63} and His^{185} in UCH-L1 (35) is involved in its interaction with LAMP-2, Hsc70, and Hsp90. We have previously reported that the R63A or H185A substitution in UCH-L1 enhances the interaction of UCH-L1 with tubulin (13). These results suggest that tubulin, LAMP-2A, Hsc70, and Hsp90 interact with the same region in UCH-L1. Arg^{63} and His^{185} are distinct from Asp^{30}, which is one of the ubiquitin-binding sites (21, 38), and from Cys^{90} (13), which is a catalytic center cysteine residue. We have shown that D30K or C90S mutation in UCH-L1 does not alter its interactions with tubulin (13) and LAMP-2 (Fig. 1*C*). Thus, the interactions of UCH-L1 with tubulin and LAMP-2 are independent of the monoubiquitin-binding and hydrolase activity of UCH-L1.

It is known that the majority of PD cases occur sporadically and that oxidative/carbonyl stresses are

elevated in PD brains (17, 39). In the brains of sporadic PD patients, UCH-L1 is a major target of carbonyl formation (17). We previously reported that carbonyl-modified UCH-L1 and UCH-L1^{I93M} share biochemical properties: both of these UCH-L1 variants display increased insolubility, elevated interactions with multiple proteins including tubulin, and decreased interaction with monoubiquitin compared with UCH-L1^{WT} (13). We have also shown that both carbonyl-modified UCH-L1 and UCH-L1^{I93M} abnormally promote tubulin polymerization (13). Our previous studies using circular dichroism suggest that both of these UCH-L1 variants display decreased α-helix and increased β-sheet content (13, 22, 40). Thus, both carbonyl modification and the I93M mutation in UCH-L1 may alter its conformation, resulting in changes in the biochemical and functional properties of UCH-L1. It is an interesting issue whether carbonyl-modified UCH-L1 can also inhibit CMA. Other than tubulin, LAMP-2A, Hsc70, and Hsp90, UCH-L1 interacts with multiple proteins (13). These other interactors may also be involved in the mechanism of UCH-L1-mediated PD and are currently under investigation. It is also possible that the interaction of Hsc70 or Hsp90 with UCH-L1 plays roles other than in the CMA pathway.

α-Synuclein and UCH-L1 have been reported to be expressed abundantly in dopaminergic neurons in the human brain (41). Thus, UCH-L1^{I93M} is possibly overproduced in dopaminergic neurons in familial PD, leading to an accumulation of α-synuclein and the selective loss of dopaminergic neurons. In conclusion, familial PD-associated mutant UCH-L1^{I93M} physically interacts with LAMP-2A, Hsc70, and Hsp90 and causes an increase in the amount of α-synuclein in cells. We propose that aberrant interaction of mutant UCH-L1 with CMA machinery, at least in part, underlies the pathogenesis of familial PD associated with UCH-L1^{I93M}.

Acknowledgments—We thank Dr. Yasuyuki Suzuki (National Institute of Neuroscience) and Dr. Rieko Setsuie (National Institute of Neuroscience) for scientific comments and Takeshi Mitsui (National Institute of Neuroscience) for technical assistance.

REFERENCES

1. Polymeropoulos, M. H., Lavedan, C., Leroy, E., Ide, S. E., Dehejia, A., Dutra, A., Pike, B., Root, H., Rubenstein, J., Boyer, R., Stenroos, E. S., Chandrasekharappa, S., Athanassiadou, A., Papapetropoulos, T., Johnson, W. G., Lazzarini, A. M., Duvoisin, R. C., Di Iorio, G., Golbe, L. I., and Nussbaum, R. L. (1997) *Science* **276,** 2045–2047
2. Kruger, R., Kuhn, W., Muller, T., Woitalla, D., Graeber, M., Kosel, S., Przuntek, H., Epplen, J. T., Schols, L., and Riess, O. (1998) *Nat. Genet.* **18,** 106–108
3. Zarranz, J. J., Alegre, J., Gomez-Esteban, J. C., Lezcano, E., Ros, R., Ampuero, I., Vidal, L., Hoenicka, J., Rodriguez, O., Atares, B., Llorens, V., Gomez Tortosa, E., del Ser, T., Munoz, D. G., and de Yebenes, J. G. (2004) *Ann. Neurol.* **55,** 164–173
4. Chartier-Harlin, M. C., Kachergus, J., Roumier, C., Mouroux, V., Douay, X., Lincoln, S., Levecque, C., Larvor, L., Andrieux, J., Hulihan, M., Waucquier, N., Defebvre, L., Amouyel, P., Farrer, M., and Destee, A. (2004) *Lancet* **364,** 1167–1169
5. Ibanez, P., Bonnet, A. M., Debarges, B., Lohmann, E., Tison, F., Pollak, P., Agid, Y., Durr, A., and Brice, A. (2004) *Lancet* **364,** 1169–1171
6. Singleton, A. B., Farrer, M., Johnson, J., Singleton, A., Hague, S., Kachergus, J., Hulihan, M., Peuralinna, T., Dutra, A., Nussbaum, R., Lincoln, S., Crawley, A., Hanson, M., Maraganore, D., Adler, C., Cookson, M. R., Muenter, M., Baptista, M., Miller, D., Blancato, J., Hardy, J., and Gwinn-Hardy, K. (2003) *Science* **302,** 841
7. Spillantini, M. G., Schmidt, M. L., Lee, V. M., Trojanowski, J. Q., Jakes, R., and Goedert, M. (1997) *Nature* **388,** 839–840
8. Spillantini, M. G., Crowther, R. A., Jakes, R., Hasegawa, M., and Goedert, M. (1998) *Proc. Natl. Acad. Sci. U. S. A.* **95,** 6469–6473
9. Leroy, E., Boyer, R., Auburger, G., Leube, B., Ulm, G., Mezey, E., Harta, G., Brownstein, M. J., Jonnalagada, S., Chernova, T., Dehejia, A., Lavedan, C., Gasser, T., Steinbach, P. J., Wilkinson, K. D., and Polymeropoulos, M. H. (1998) *Nature* **395,** 451–452
10. Setsuie, R., and Wada, K. (2007) *Neurochem. Int.* **51,** 105–111
11. Healy, D. G., Abou-Sleiman, P. M., and Wood, N. W. (2004) *Cell Tissue Res.* **318,** 189–194
12. Setsuie, R., Wang, Y. L., Mochizuki, H., Osaka, H., Hayakawa, H., Ichihara, N., Li, H., Furuta, A., Sano, Y., Sun, Y. J., Kwon, J., Kabuta, T., Yoshimi, K., Aoki, S., Mizuno, Y., Noda, M., and Wada, K. (2007) *Neurochem. Int.* **50,** 119–129
13. Kabuta, T., Setsuie, R., Mitsui, T., Kinugawa, A., Sakurai, M., Aoki, S., Uchida, K., and Wada, K. (2008) *Hum. Mol. Genet.* **17,** 1482–1496
14. Lowe, J., McDermott, H., Landon, M., Mayer, R. J., and Wilkinson, K. D. (1990) *J. Pathol.* **161,** 153–160
15. Maraganore, D. M., Lesnick, T. G., Elbaz, A., Chartier-Harlin, M. C., Gasser, T., Kruger, R., Hattori, N., Mellick, G. D., Quattrone, A., Satoh, J., Toda, T., Wang, J., Ioannidis, J. P., de Andrade, M., and Rocca, W. A. (2004) *Ann. Neurol.* **55,** 512–521
16. Healy, D. G., Abou-Sleiman, P. M., Casas, J. P., Ahmadi, K. R., Lynch, T., Gandhi, S., Muqit, M. M., Foltynie, T., Barker, R., Bhatia, K. P., Quinn, N. P., Lees, A. J., Gibson, J. M., Holton, J. L., Revesz, T., Goldstein, D. B., and Wood, N. W. (2006) *Ann. Neurol.* **59,** 627–633
17. Choi, J., Levey, A. I., Weintraub, S. T., Rees, H. D., Gearing, M., Chin, L. S., and Li, L. (2004) *J. Biol. Chem.* **279,** 13256–13264
18. Wilkinson, K. D., Lee, K. M., Deshpande, S., Duerksen-Hughes, P., Boss, J. M., and Pohl, J. (1989) *Science* **246,** 670–673
19. Larsen, C. N., Krantz, B. A., and Wilkinson, K. D. (1998) *Biochemistry* **37,** 3358–3368
20. Liu, Y., Fallon, L., Lashuel, H. A., Liu, Z., and Lansbury, P. T., Jr. (2002) *Cell* **111,** 209–218
21. Osaka, H., Wang, Y. L., Takada, K., Takizawa, S., Setsuie, R., Li, H., Sato, Y., Nishikawa, K., Sun, Y. J., Sakurai, M., Harada, T., Hara, Y., Kimura, I., Chiba, S., Namikawa, K., Kiyama, H., Noda, M., Aoki, S., and Wada, K. (2003) *Hum. Mol. Genet.* **12,** 1945–1958
22. Nishikawa, K., Li, H., Kawamura, R., Osaka, H., Wang, Y. L., Hara, Y., Hirokawa, T., Manago, Y., Amano, T., Noda, M., Aoki, S., and Wada, K. (2003) *Biochem. Biophys. Res. Commun.* **304,** 176–183
23. Saigoh, K., Wang, Y. L., Suh, J. G., Yamanishi, T., Sakai, Y., Kiyosawa, H., Harada, T., Ichihara, N., Wakana, S., Kikuchi, T., and Wada, K. (1999) *Nat. Genet.* **23,** 47–51
24. Cuervo, A. M., Stefanis, L., Fredenburg, R., Lansbury, P. T., and Sulzer, D. (2004) *Science* **305,** 1292–1295
25. Cuervo, A. M. (2004) *Trends Cell Biol.* **14,** 70–77
26. Agarraberes, F. A., and Dice, J. F. (2001) *J. Cell Sci.* **114,** 2491–2499
27. Finn, P. F., and Dice, J. F. (2005) *J. Biol. Chem.* **280,** 25864–25870
28. Kabuta, T., Suzuki, Y., and Wada, K. (2006) *J. Biol. Chem.* **281,** 30524–30533
29. Pertoft, H., Warmegard, B., and Hook, M. (1978) *Biochem. J.* **174,** 309–317
30. Kabuta, T., Hakuno, F., Asano, T., and Takahashi, S. (2002) *J. Biol. Chem.* **277,** 6846–6851
31. Eskelinen, E. L., Cuervo, A. M., Taylor, M. R., Nishino, I., Blum, J. S., Dice, J. F., Sandoval, I. V., Lippincott-Schwartz, J., August, J. T., and Saftig, P. (2005) *Traffic* **6,** 1058–1061
32. Dice, J. F. (1990) *Trends Biochem. Sci.* **15,** 305–309
33. Levine, B., and Kroemer, G. (2008) *Cell* **132,** 27–42
34. Webb, J. L., Ravikumar, B., Atkins, J., Skepper, J. N., and Rubinsztein, D. C. (2003) *J. Biol. Chem.* **278,** 25009–25013
35. Das, C., Hoang, Q. Q., Kreinbring, C. A., Luchansky, S. J., Meray, R. K., Ray, S. S., Lansbury, P. T., Ringe, D., and Petsko, G. A. (2006) *Proc. Natl. Acad.*

Sci. U. S. A. **103,** 4675–4680
36. Majeski, A. E., and Dice, J. F. (2004) *Int. J. Biochem. Cell Biol.* **36,** 2435–2444
37. Baba, M., Nakajo, S., Tu, P. H., Tomita, T., Nakaya, K., Lee, V. M., Trojanowski, J. Q., and Iwatsubo, T. (1998) *Am. J. Pathol.* **152,** 879–884
38. Johnston, S. C., Riddle, S. M., Cohen, R. E., and Hill, C. P. (1999) *EMBO J.* **18,** 3877–3887
39. Ischiropoulos, H., and Beckman, J. S. (2003) *J. Clin. Investig.* **111,** 163–169
40. Naito, S., Mochizuki, H., Yasuda, T., Mizuno, Y., Furusaka, M., Ikeda, S., Adachi, T., Shimizu, H. M., Suzuki, J., Fujiwara, S., Okada, T., Nishikawa, K., Aoki, S., and Wada, K. (2006) *Biochem. Biophys. Res. Commun.* **339,** 717–725
41. Solano, S. M., Miller, D. W., Augood, S. J., Young, A. B., and Penney, J. B., Jr. (2000) *Ann. Neurol.* **47,** 201–210

[Autophagy 4:6, 827-829; 16 August 2008]; ©2008 Landes Bioscience

Article Addendum

Insights into links between familial and sporadic Parkinson's disease

Physical relationship between UCH-L1 variants and chaperone-mediated autophagy

Tomohiro Kabuta and Keiji Wada

Department of Degenerative Neurological Diseases; National Institute of Neuroscience; National Center of Neurology and Psychiatry; Kodaira, Tokyo, Japan

Abbreviations: UCH-L1, ubiquitin C-terminal hydrolase L1; PD, Parkinson's disease; CMA, chaperone-mediated autophagy; WT, wild-type; LAMP-2, lysosome-associated membrane protein type 2; Hsc70, heat shock cognate protein 70; Hsp90, heat shock protein 90; GAPDH, glyceraldehyde-3-phosphate dehydrogenase; HAE, 4-hydroxy-2-alkenals; HNE, 4-hydroxy-2-nonenal

Key words: ubiquitin C-terminal hydrolase L1 (UCH-L1), Parkinson's disease, LAMP-2, chaperone-mediated autophagy, α-synuclein

Ubiquitin C-terminal hydrolase L1 (UCH-L1) is expressed abundantly in neurons and has been reported to be a major target of oxidative/carbonyl damage associated with sporadic Parkinson's disease (PD). The I93M mutation in UCH-L1 is also associated with familial PD. We recently reported that UCH-L1 physically interacts with LAMP-2A, the lysosomal receptor for chaperone-mediated autophagy (CMA), and Hsc70 and Hsp90, both of which can function as components of the CMA pathway. We found that the levels of these interactions were aberrantly increased by the I93M mutation, and that expression of I93M UCH-L1 in cells induced the CMA inhibition-associated increase in the amount of α-synuclein, a risk factor for PD. The interactions of UCH-L1 with LAMP-2A, Hsc70 and Hsp90 were also abnormally enhanced by carbonyl modification of UCH-L1. We propose that aberrant interactions of UCH-L1 variants with CMA machinery, at least partly, underlie the pathogenesis of I93M UCH-L1-associated PD, and possibly of sporadic PD. Our findings may provide novel insights into the links between familial and sporadic PD.

Parkinson's disease (PD) is the most common neurodegenerative movement disorder. It is characterized by progressive cell loss of dopaminergic neurons in the substantia nigra pars compacta. A missense mutation in the ubiquitin C-terminal hydrolase L1 (UCH-L1) gene, leading to an I93M substitution at the amino acid residue level, has been reported in a German family with dominantly inherited PD.[1] We have previously shown that I93M UCH-L1-transgenic mice exhibit progressive cell loss of dopaminergic neurons.[2] Compared with wild-type (WT) UCH-L1, I93M UCH-L1 displays increased insolubility and levels of interactions with other proteins in mammalian cells, features that are characteristic of several neurodegenerative disease-linked mutants.[3] These findings suggest that the I93M mutation in UCH-L1 is a causative mutation for PD. Although the binding of I93M UCH-L1 to monoubiquitin as well as the hydrolase activity of I93M UCH-L1 are decreased compared with those of WT UCH-L1,[1,3,4] mice deficient in UCH-L1 do not display obvious dopaminergic cell loss.[5,6] Thus, the main cause of I93M UCH-L1-associated PD may not be a loss of UCH-L1 function but an acquired toxicity of I93M UCH-L1. Our previous studies suggest that aberrantly enhanced physical interactions between I93M UCH-L1 and multiple proteins, including tubulin, underlie the toxic functions of I93M UCH-L1 (Fig. 1).[3]

Several missense mutations in the α-synuclein gene are also linked to dominant-inherited PD.[7-9] α-Synuclein is thought to be a major component of cytoplasmic inclusions called Lewy bodies in the brains of patients with sporadic PD.[10,11] Increases in the levels of α-synuclein could constitute a cause of PD, since duplication and triplication of the α-synuclein gene cause familial PD or parkinsonism.[12-14] α-Synuclein is degraded at least partly by chaperone-mediated autophagy (CMA).[15]

To elucidate the molecular relationship between α-synuclein and UCH-L1 in the pathogenesis of PD, we sought to identify novel UCH-L1-interacting proteins. We found that UCH-L1 interacts with lysosome-associated membrane protein type 2A (LAMP-2A), heat shock cognate protein 70 (Hsc70) and heat shock protein 90 (Hsp90),[16] all of which are components of the CMA pathway.[17] These interactions were enhanced by the I93M mutation in UCH-L1.[16] Expression of I93M UCH-L1 in cells induced the increase in the amount of α-synuclein and glyceraldehyde-3-phosphate dehydrogenase (GAPDH),[16] both of which are substrates of CMA,[15] but had almost no effects on the amount of ΔDQ α-synuclein,[16] which lacks the CMA recognition motif.[15] Based on these results, we propose that the aberrant interaction of I93M UCH-L1 with CMA machinery causes the accumulation of α-synuclein and GAPDH by inhibiting CMA. Besides its role in glycolysis, GAPDH is known to initiate a cell-death cascade.[18] Thus, it is possible that the increases in

Correspondence to: Tomohiro Kabuta or Keiji Wada; Department of Degenerative Neurological Diseases; National Institute of Neuroscience; National Center of Neurology and Psychiatry; 4-1-1 Ogawahigashi; Kodaira, Tokyo 187-8502 Japan; Tel.: +81.42.346.1715; Fax: +81.42.346.1745; Email: kabuta@ncnp.go.jp or wada@ncnp.go.jp

Submitted: 07/03/08; Revised: 07/08/08; Accepted: 07/08/08

Previously published online as an *Autophagy* E-publication: www.landesbioscience.com/journals/autophagy/article/6560

Addendum to: Kabuta T, Furuta A, Aoki S, Furuta K, Wada K. Aberrant interaction between Parkinson disease-associated mutant UCH-L1 and the lysosomal receptor for chaperone-mediated autophagy. J Biol Chem 2008; Epub ahead of print.

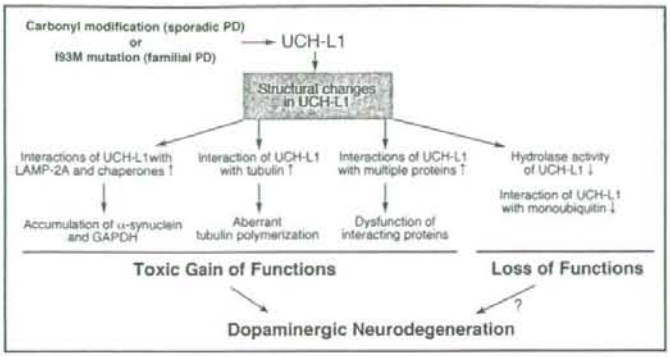

Figure 1. Possible role of UCH-L1 in PD. The I93M mutation (as occurs in familial PD associated with I93M UCH-L1) and carbonyl-modification (as occurs in sporadic PD) cause structural changes in UCH-L1. The hydrolase activity and binding affinity to monoubiquitin of these UCH-L1 proteins are decreased. The involvement of loss of UCH-L1 functions in the pathogenesis of PD is currently unclear. Abnormal UCH-L1 interacts tightly with LAMP-2A, Hsc70 and Hsp90. These abnormal UCH-L1 may inhibit CMA-dependent degradation, and cause CMA substrates including α-synuclein and GAPDH to accumulate. The increased amount of α-synuclein or GAPDH proteins possibly contributes to the neurodegeneration of dopaminergic neurons. The aberrant interactions of UCH-L1 with other proteins, including tubulin, may also contribute to neurodegeneration. ↑: increase compared with wild-type UCH-L1, ↓: decrease compared with wild-type UCH-L1.

the amount of α-synuclein and GAPDH are involved in the pathogenesis of PD (Fig. 1).

Although the majority of PD cases occur sporadically, the molecular mechanisms that underlie the pathology of sporadic PD are poorly understood. It is known that oxidative/carbonyl stresses are elevated in PD brains.[19,20] In the brains of sporadic PD patients, UCH-L1 is a major target of carbonyl formation,[19] which is the most widely used marker for oxidative damage to proteins. Carbonyl groups can be introduced into proteins in vivo mainly by reactions with 2-alkenals, 4-hydroxy-2-alkenals (HAE) or ketoaldehydes,[21,22] which are endogenous aldehyde products formed by lipid peroxidation or glycooxidation. Protein carbonyls can also be produced by metal-catalyzed reactions with H_2O_2 in vitro.[22,23] It has been suggested that 4-hydroxy-2-nonenal (HNE) can accumulate in biological membranes at concentrations of over 10–100 μM in response to oxidative stress.[24,25] In mammalian cells, carbonyl-modified UCH-L1 can be produced by reactions with 10–100 μM HAE or 2-alkenals, but not by 100–500 μM ketoaldehydes or 0.1–1 mM H_2O_2.[3] Furthermore, I93M UCH-L1 and carbonyl-modified UCH-L1 display shared aberrant properties,[3] suggesting that carbonyl-modified UCH-L1 constitutes one of the causes of sporadic PD. Therefore, we tested the effects of carbonyl modification of UCH-L1 on the interaction of UCH-L1 with LAMP-2A and chaperones. We found that HNE modification of UCH-L1 promotes interactions between UCH-L1 and LAMP-2A, Hsc70 or Hsp90 (Fig. 2A). 4-hydroxy-2-hexenal or 2-propenal modification of UCH-L1 have similar effects on the interactions between UCH-L1 and LAMP-2A, Hsc70 or Hsp90 as HNE modification (data not shown). In a pull-down assay, HNE-modified UCH-L1 exhibits an abnormally increased level of interaction with the cytosolic region of LAMP-2A, compared with wild-type UCH-L1 (data not shown). Thus, I93M UCH-L1 and carbonyl-modified UCH-L1 also exhibit common biochemical properties with respect to their interactions with LAMP-2A, Hsc70 and Hsp90. These results support the idea that carbonyl-modified UCH-L1 constitutes one of the causes of sporadic PD (Fig. 1). A coimmunoprecipitation assay using C90S, C132S and C152S UCH-L1 mutants shows less binding of C90S UCH-L1 to LAMP-2A, Hsc70 or Hsp90 than WT UCH-L1, when cells are treated with HNE (Fig. 2B and C). Thus, HNE modification of Cys-90 of UCH-L1 promotes the interactions of UCH-L1 with LAMP-2A, Hsc70 and Hsp90. These results are consistent with our previous data showing that the HAE modification of Cys-90 of UCH-L1 promotes the interactions of UCH-L1 with multiple proteins.[3]

The appearance of HNE-modified proteins in nigral neurons is associated with sporadic PD.[26,27] We have previously observed that cysteine residues in UCH-L1 are main targets for HNE-modification of UCH-L1.[3] UCH-L1 is modified by 10–100 μM HNE, whereas α-synuclein, which contains no cysteine residues, is not modified by 100 μM HNE in mammalian cells,[3] suggesting that, in mammalian cells, HNE reacts with proteins mainly via cysteine residues. It is possible that, in sporadic PD, cysteine residue-reactive carbonyl stresses such as HAE result in the accumulation of α-synuclein, not by direct modification of α-synuclein, but via reaction with UCH-L1.

In conclusion, aberrant interactions of UCH-L1 variants with multiple proteins, including CMA machinery, may underlie the pathogenesis of I93M UCH-L1-associated PD, and possibly of sporadic PD. We propose that carbonyl modification of UCH-L1 can be a therapeutic target for the treatment of sporadic PD.

References

1. Leroy E, Boyer R, Auburger G, Leube B, Ulm G, Mezey E, Harta G, Brownstein MJ, Jonnalagada S, Chernova T, Dehejia A, Lavedan C, Gasser T, Steinbach PJ, Wilkinson KD, Polymeropoulos MH. The ubiquitin pathway in Parkinson's disease. Nature 1998; 395:451-2.
2. Setsuie R, Wang YL, Mochizuki H, Osaka H, Hayakawa H, Ichihara N, Li H, Furuta A, Sano Y, Sun YJ, Kwon J, Kabuta T, Yoshimi K, Aoki S, Mizuno Y, Noda M, Wada K. Dopaminergic neuronal loss in transgenic mice expressing the Parkinson's disease-associated UCH-L1 I93M mutant. Neurochem Int 2007; 50:119-29.
3. Kabuta T, Setsuie R, Mitsui T, Kinugawa A, Sakurai M, Aoki S, Uchida K, Wada K. Aberrant molecular properties shared by familial Parkinson's disease-associated mutant UCH-L1 and carbonyl-modified UCH-L1. Hum Mol Genet 2008; 17:1482-96.
4. Nishikawa K, Li H, Kawamura R, Osaka H, Wang YL, Hara Y, Hirokawa T, Manago Y, Amano T, Noda M, Aoki S, Wada K. Alterations of structure and hydrolase activity of parkinsonism-associated human ubiquitin carboxyl-terminal hydrolase L1 variants. Biochem Biophys Res Commun 2003; 304:176-83.
5. Saigoh K, Wang YL, Suh JG, Yamanishi T, Sakai Y, Kiyosawa H, Harada T, Ichihara N, Wakana S, Kikuchi T, Wada K. Intragenic deletion in the gene encoding ubiquitin carboxy-terminal hydrolase in gad mice. Nat Genet 1999; 23:47-51.
6. Osaka H, Wang YL, Takada K, Takizawa S, Setsuie R, Li H, Sato Y, Nishikawa K, Sun YJ, Sakurai M, Harada T, Hara Y, Kimura I, Chiba S, Namikawa K, Kiyama H, Noda M, Aoki S, Wada K. Ubiquitin carboxy-terminal hydrolase L1 binds to and stabilizes monoubiquitin in neuron. Hum Mol Genet 2003; 12:1945-58.
7. Polymeropoulos MH, Lavedan C, Leroy E, Ide SE, Dehejia A, Dutra A, Pike B, Root H, Rubenstein J, Boyer R, Stenroos ES, Chandrasekharappa S, Athanassiadou A, Papapetropoulos T, Johnson WG, Lazzarini AM, Duvoisin RC, Di Iorio G, Golbe LI, Nussbaum RL. Mutation in the α-synuclein gene identified in families with Parkinson's disease. Science 1997; 276:2045-7.

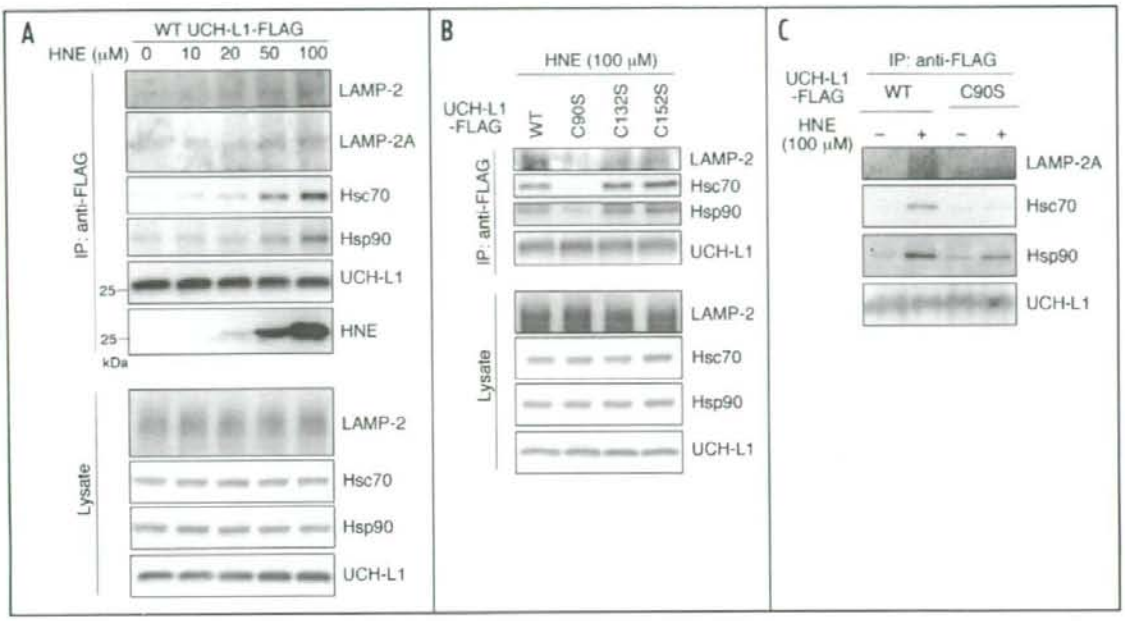

Figure 2. Effects of HNE-modification of UCH-L1 on the interactions of UCH-L1 with LAMP-2A, Hsc70 and Hsp90 (A) COS-7 cells transfected with FLAG-tagged WT UCH-L1 were treated with the indicated concentrations of HNE. Lysates were immunoprecipitated with anti-FLAG antibody, and analyzed by immunoblotting using anti-LAMP-2, LAMP-2A, Hsc70, Hsp90, HNE and FLAG antibodies. (B and C) COS-7 cells transfected with the indicated constructs were treated with or without 100 μM HNE. Lysates were immunoprecipitated using anti-FLAG antibody, and analyzed by immunoblotting.

8. Kruger R, Kuhn W, Muller T, Woitalla D, Graeber M, Kosel S, Przuntek H, Epplen JT, Schols L, Riess O. Ala30Pro mutation in the gene encoding alpha-synuclein in Parkinson's disease. Nat Genet 1998; 18:106-8.
9. Zarranz JJ, Alegre J, Gomez-Esteban JC, Lezcano E, Ros R, Ampuero I, Vidal L, Hoenicka J, Rodriguez O, Atares B, Llorens V, Gomez Tortosa E, del Ser T, Munoz DG, de Yebenes JG. The new mutation, E46K, of α-synuclein causes Parkinson and Lewy body dementia. Ann Neurol 2004; 55:164-73.
10. Spillantini MG, Schmidt ML, Lee VM, Trojanowski JQ, Jakes R, Goedert M. Alpha-synuclein in Lewy bodies. Nature 1997; 388:839-40.
11. Spillantini MG, Crowther RA, Jakes R, Hasegawa M, Goedert M. alpha-Synuclein in filamentous inclusions of Lewy bodies from Parkinson's disease and dementia with lewy bodies. Proc Natl Acad Sci USA 1998; 95:6469-73.
12. Chartier-Harlin MC, Kachergus J, Roumier C, Mouroux V, Douay X, Lincoln S, Levecque C, Larvor L, Andrieux J, Hulihan M, Waucquier N, Defebvre L, Amouyel P, Farrer M, Destee A. α-synuclein locus duplication as a cause of familial Parkinson's disease. Lancet 2004; 364:1167-9.
13. Ibanez P, Bonnet AM, Debarges B, Lohmann E, Tison F, Pollak P, Agid Y, Durr A, Brice A. Causal relation between α-synuclein gene duplication and familial Parkinson's disease. Lancet 2004; 364:1169-71.
14. Singleton AB, Farrer M, Johnson J, Singleton A, Hague S, Kachergus J, Hulihan M, Peuralinna T, Dutra A, Nussbaum R, Lincoln S, Crawley A, Hanson M, Maraganore D, Adler C, Cookson MR, Muenter M, Baptista M, Miller D, Blancato J, Hardy J, Gwinn-Hardy K. α-Synuclein locus triplication causes Parkinson's disease. Science 2003; 302:841.
15. Cuervo AM, Stefanis L, Fredenburg R, Lansbury PT, Sulzer D. Impaired degradation of mutant α-synuclein by chaperone-mediated autophagy. Science 2004; 305:1292-5.
16. Kabuta T, Furuta A, Aoki S, Furuta K, Wada K. Aberrant interaction between Parkinson disease-associated mutant UCH-L1 and the lysosomal receptor for chaperone-mediated autophagy. J Biol Chem 2008; Epub ahead of print.
17. Agarraberes FA, Dice JF. A molecular chaperone complex at the lysosomal membrane is required for protein translocation. J Cell Sci 2001; 114:2491-9.
18. Sen N, Hara MR, Kornberg MD, Cascio MB, Bae BI, Shahani N, Thomas B, Dawson TM, Dawson VL, Snyder SH, Sawa A. Nitric oxide-induced nuclear GAPDH activates p300/CBP and mediates apoptosis. Nat Cell Biol 2008; 10:866-73.
19. Choi J, Levey AI, Weintraub ST, Rees HD, Gearing M, Chin LS, Li L. Oxidative modifications and down-regulation of ubiquitin carboxyl-terminal hydrolase L1 associated with idiopathic Parkinson's and Alzheimer's diseases. J Biol Chem 2004; 279:13256-64.
20. Ischiropoulos H, Beckman JS. Oxidative stress and nitration in neurodegeneration: cause, effect, or association? J Clin Invest 2003; 111:163-9.
21. Uchida K. Role of reactive aldehyde in cardiovascular diseases. Free Radic Biol Med 2000; 28:1685-96.
22. Uchida K. Histidine and lysine as targets of oxidative modification. Amino Acids 2003; 25:249-57.
23. Stadtman ER. Oxidation of free amino acids and amino acid residues in proteins by radiolysis and by metal-catalyzed reactions. Annu Rev Biochem 1993; 62:797-821.
24. Uchida K. 4-Hydroxy-2-nonenal: a product and mediator of oxidative stress. Prog Lipid Res 2003; 42:318-43.
25. Esterbauer H, Schaur RJ, Zollner H. Chemistry and biochemistry of 4-hydroxynonenal, malonaldehyde and related aldehydes. Free Radic Biol Med 1991; 11:81-128.
26. Yoritaka A, Hattori N, Uchida K, Tanaka M, Stadtman ER, Mizuno Y. Immunohistochemical detection of 4-hydroxynonenal protein adducts in Parkinson disease. Proc Natl Acad Sci USA 1996; 93:2696-701.
27. Castellani RJ, Perry G, Siedlak SL, Nunomura A, Shimohama S, Zhang J, Montine T, Sayre LM, Smith MA. Hydroxynonenal adducts indicate a role for lipid peroxidation in neocortical and brainstem Lewy bodies in humans. Neurosci Lett 2002; 319:25-8.